

Suppression of the neutralino relic density with supersymmetric CP violation

Takeshi Nihei*

Department of Physics, College of Science and Technology,

Nihon University, 1-8-14, Kanda-Surugadai,

Chiyoda-ku, Tokyo, 101-8308, Japan

Abstract

We study pair annihilations of the neutralino dark matter in the minimal supersymmetric standard model with CP violation. We consider the case that the higgsino mass and the trilinear scalar couplings have CP-violating phases of order unity, taking a scenario that the scalar fermions in the first two generations are much heavier than those in the third generation to avoid a severe constraint from experimental limits on electric dipole moments. It is found that, when the lightest neutralino (χ) is bino-like, the cross sections of the W -boson pair production $\chi\chi \rightarrow W^+W^-$ and the lightest Higgs boson pair production $\chi\chi \rightarrow H_2^0 H_2^0$ for nonrelativistic neutralinos can be significantly enhanced by the phase of the higgsino mass. The relic density of the neutralino can be considerably suppressed by this effect. However, even this suppression is not enough to make bino-like dark matter consistent with a cosmological constraint. We also discuss the effect of CP violation on the positron flux from neutralino pair annihilations in the galactic halo.

*Electronic address: nihei@phys.cst.nihon-u.ac.jp

I. INTRODUCTION

Existence of a considerable amount of cold dark matter (CDM) in the present Universe has been regarded as a robust ingredient in recent astrophysics and cosmology [1]. In particular, the Wilkinson Microwave Anisotropy Probe (WMAP) has determined the relic abundance of CDM as [2]

$$\Omega_{\text{CDM}} h^2 = 0.1126^{+0.008}_{-0.009}, \quad (1)$$

where Ω_{CDM} is the CDM energy density normalized by the critical density and $h \approx 0.7$ is the Hubble constant in units of 100 km/sec/Mpc [3]. The relic density of the CDM is expected to be determined with more accuracy by analyses of increasing WMAP data and forthcoming data from the future project Planck [4].

Identification of the CDM as a particle still remains to be settled. Among possible candidates, the lightest superparticle (LSP) in supersymmetric models is one of the most attractive candidates [5, 6]. In supersymmetric models, conservation of a discrete symmetry called R-parity is necessary to avoid rapid proton decay, but it in turn plays a crucial role to guarantee the stability of the LSP. In the minimal supersymmetric standard model (MSSM) [7], the LSP is typically the lightest neutralino [8] which is a linear combination of neutral gauginos and higgsinos

$$\chi = \chi_1^0 = N_{11}\tilde{B} + N_{12}\tilde{W}^3 + N_{13}\tilde{H}_1^0 + N_{14}\tilde{H}_2^0, \quad (2)$$

where \tilde{B} is the $U(1)_Y$ gaugino (bino), \tilde{W}^3 is the neutral $SU(2)_L$ gaugino (wino), and \tilde{H}_1^0 and \tilde{H}_2^0 are the two neutral higgsinos with opposite hypercharges. The coefficients N_{1i} ($i = 1, 2, 3, 4$) are the elements of the 4×4 unitary matrix N which diagonalizes the neutralino mass matrix [7].

A number of theoretical analyses on the relic density of the neutralino CDM in the MSSM have already been done extensively [9, 10, 11, 12, 13, 14, 15, 16, 17, 18, 19]. However, most analyses have been done with an assumption of no CP violation in supersymmetric parameters. CP violation is not only observed in particle physics but also expected to play an essential role to explain baryon asymmetry in the Universe.

Since it is known that the standard source of CP violation in the Cabibbo–Kobayashi–Maskawa mixing matrix is not enough to produce required asymmetry of order 10^{-10} , supersymmetric CP violation is expected to generate the correct amount of baryon asymmetry [20, 21]. Thus, it is generically important to include the effect of supersymmetric CP violation. When the supersymmetric CP phases are of order unity, they typically lead to too large electric dipole moments of the neutron, the electron and ^{199}Hg atom to satisfy experimental limits [22, 23, 24] if masses of superparticles are within a TeV scale. However, if superparticles in the first two generations are much heavier than 1 TeV, the supersymmetric CP phases of order unity are still allowed.

On the other hand, a complete analysis of the neutralino relic density $\Omega_\chi h^2$ including all the relevant effects in the MSSM with CP violation is still missing. The effect of CP violation on the neutralino pair annihilation cross section into the fermion pairs through the sfermion exchange was studied in Ref. [25]. In Ref. [26], the effects of a CP-violating phase in the trilinear scalar couplings on the neutralino pair annihilation cross section were examined, including all the final states and taking into account the scalar and pseudoscalar mixing in the neutral Higgs sector [27, 28]. Recently, the dependence of $\Omega_\chi h^2$ on CP-violating phases through supersymmetric loop corrections to the bottom-quark mass was examined in Ref. [29]. Partial wave treatment in the presence of CP violation was studied in Ref. [30]. An analysis related with electroweak baryogenesis was done in Ref. [31].

In this paper, we extend our previous analysis [32] and perform a reanalysis on the effects of CP-violating complex phases in the MSSM on pair annihilation cross sections of the lightest neutralino and its relic density in the present Universe. We consider the case that the higgsino mass and the trilinear scalar couplings have CP-violating phases of order unity, taking a scenario that the scalar fermions in the first two generations are much heavier than those in the third generation to avoid a severe constraint from experimental limits on electric dipole moments. We include all the contributions to the neutralino annihilation cross section at the tree level, taking into account the scalar and pseudoscalar mixing in the neutral Higgs sector. In the absence

of CP violation, it is known that fermion pair productions $\chi\chi \rightarrow f\bar{f}$ usually give the largest contribution to the total cross section for a bino-like LSP. In the present paper, we shall show that, unlike the case without CP violation, the W -boson pair production $\chi\chi \rightarrow W^+W^-$ or the lightest Higgs boson pair production $\chi\chi \rightarrow H_2^0 H_2^0$ can give the largest contribution in the presence of CP violation. We also discuss the effect of CP violation on the positron flux from neutralino pair annihilations in the galactic halo.

This paper is organized as follows. In section II, we describe the structure of the MSSM with supersymmetric CP violation, and present the relevant interactions. In section III, we discuss the effect of CP violation on the cross section of the lightest neutralino pair annihilation. In section IV, we briefly review the formalism to compute the relic density of the neutralino. In section V, we summarize the procedure to obtain the positron flux. In section VI, we present our numerical results. Finally concluding remarks are given in Section VII.

II. THE MSSM WITH SUPERSYMMETRIC CP VIOLATION

In the present work, we consider a general MSSM [7] in which all the interactions are specified by the following input parameters at the weak scale

$$M_1, M_2, M_3, \mu, m_0, A, \tan\beta, m_A, \quad (3)$$

where M_1 , M_2 and M_3 are the mass parameters for the bino, the wino and the gluino, respectively. The parameter μ represents the Higgs mixing mass, and m_0 is the supersymmetry breaking common mass parameter for the sfermions in the third generation. The corresponding mass parameters for the first two generations are assumed to be 10 TeV to suppress the electric dipole moments¹. The parameter A is the common trilinear scalar coupling for the third generation, while the ones for the first two generations are neglected. The ratio of the vacuum expectation values of the two neutral

¹ The sfermion mass spectrum considered here naturally arises in a minimal supersymmetric $SO(10)$ GUT model [33].

Higgs fields is denoted by $\tan\beta$. The quantity m_A is a parameter which coincides with the pseudoscalar Higgs mass in the absence of CP violation [27, 28]. In eq. (3), M_i ($i = 1, 2, 3$), μ and A can have CP-violating phases in general. For the gaugino masses, we assume the GUT relation

$$\frac{3}{5} \frac{M_1}{g'^2} = \frac{M_2}{g^2} = \frac{M_3}{g_s^2}, \quad (4)$$

where g' , g and g_s are the gauge coupling constants for $U(1)_Y$, $SU(2)_L$ and $SU(3)_C$ gauge groups, respectively. With this relation, the neutralino LSP can be bino-like ($|M_1| \ll |\mu|$), higgsino-like ($|M_1| \gg |\mu|$) or their mixture ($|M_1| \approx |\mu|$).

In the present analysis, we assume that the gaugino masses M_i are real, and examine the effects of the CP-violating phases of μ and A

$$\mu = |\mu| \exp(i\theta_\mu), \quad A = |A| \exp(i\theta_A). \quad (5)$$

These phases induce imaginary parts in the mass matrices for the neutralinos, the charginos and the sfermions. They also induce mixings between scalar Higgs fields and a pseudoscalar Higgs field through radiative corrections [27, 28]. The MSSM contains two scalar neutral Higgses ϕ_1^0 and ϕ_2^0 with hypercharges $\frac{Y}{2}(\phi_1^0) = -\frac{Y}{2}(\phi_2^0) = -\frac{1}{2}$ and a pseudoscalar neutral Higgs A^0 as physical fields. In general, nonzero phases in μ or A induce ϕ_1^0 - A^0 and ϕ_2^0 - A^0 mixings at the one-loop level, so that the 3×3 mass-squared matrix \mathcal{M}_H^2 for the neutral Higgs fields has to be diagonalized. We calculate the Higgs mass-squared matrix with the one-loop effective potential, including the contributions of the third generation fermions and sfermions. The mass eigenstates H_r^0 ($r = 1, 2, 3$) are related with the CP eigenstates $(\phi_1^0, \phi_2^0, A^0)$ by a 3×3 rotation matrix O as follows

$$\begin{pmatrix} H_1^0 \\ H_2^0 \\ H_3^0 \end{pmatrix} = O \begin{pmatrix} \phi_1^0 \\ \phi_2^0 \\ A^0 \end{pmatrix}. \quad (6)$$

The Higgs boson mass eigenvalues are obtained as $O\mathcal{M}_H^2O^T = \text{diag}(m_{H_1^0}^2, m_{H_2^0}^2, m_{H_3^0}^2)$. In eq. (6), H_2^0 is defined as the lightest Higgs. The heavier Higgses H_1^0 and H_3^0 are

defined such that $|O_{13}| \leq |O_{33}|$. In the case of $\theta_\mu = \theta_A = 0$, it follows that H_1^0 (H_2^0) is the heavier (lighter) scalar Higgs field, and H_3^0 is the pseudoscalar Higgs field. Note that the parameter m_A in eq. (3) is not a mass eigenvalue in general. The scalar–pseudoscalar mixing in the neutral Higgs sector implies $O_{r3} \neq 0$ ($r = 1, 2$) so that interactions of the neutral Higgs bosons are significantly modified [27, 28].

Our phase convention in the Higgs sector is defined as follows. In addition to θ_μ and θ_A , the coefficient of a Higgs mixing term ($\phi_1^0 \phi_2^0$) can have a complex phase θ_{12} (See Ref. [27]). In general these phases induce a nonvanishing relative phase ξ between the vacuum expectation values of the two Higgs fields through the relevant tadpole minimum condition. However, θ_{12} and ξ are not separately physical quantities, and only their sum $\xi + \theta_{12}$ is rephasing invariant. We adopt a convention that $\xi = 0$ at the one-loop level so that nonvanishing θ_{12} will be induced by the tadpole condition in the presence of nonvanishing θ_μ or θ_A .

In the present work, we focus on the W -boson pair production $\chi\chi \rightarrow W^+W^-$ and the lightest Higgs boson pair production $\chi\chi \rightarrow H_2^0 H_2^0$. For later discussion, we explicitly describe the structure of the interactions relevant for these processes in the following.

When the Higgsino mass μ has a nonvanishing phase, the elements of the neutralino mixing matrix N have an imaginary part in general. The interactions of the neutral Higgses with the neutralinos χ_i^0 ($i = 1, 2, 3, 4$) in the presence of CP violation have the following structure

$$\mathcal{L}_{\chi^0 \chi^0 H^0} = \frac{1}{2} \sum_{r=1}^3 \sum_{i,j=1}^4 \bar{\chi}_i^0 \left(C_S^{\chi_i^0 \chi_j^0 H_r^0} - C_P^{\chi_i^0 \chi_j^0 H_r^0} \gamma_5 \right) \chi_j^0 H_r^0. \quad (7)$$

In the absence of CP violation, either the scalar coupling C_S or the pseudoscalar coupling C_P in eq. (7) is vanishing for every mass eigenstate H_r^0 [7]. Namely, the scalar coupling C_S is vanishing for H_3^0 , and the pseudoscalar coupling C_P is vanishing for H_1^0 and H_2^0 . In the presence of CP violation, however, both C_S and C_P are nonzero for every mass eigenstate. These couplings can be written as

$$C_S^{\chi_i^0 \chi_j^0 H_r^0} = \text{Re}(G_r^{ij}),$$

$$C_P^{\chi_i^0 \chi_j^0 H_r^0} = i \operatorname{Im}(G_r^{ij}), \quad (8)$$

where

$$G_r^{ij} = \frac{1}{2}(g' N_{i1} - g N_{i2})[N_{j3} O_{r1} - N_{j4} O_{r2} + i O_{r3}(N_{j3} \sin \beta - N_{j4} \cos \beta)] + (i \leftrightarrow j). \quad (9)$$

Note that the couplings in eq. (8) are vanishing if the lightest neutralino χ ($= \chi_1^0$) is a pure bino or a pure higgsino. However, such a case can not take place in practice since there always exists a finite mixing between the bino and the higgsino.

The W -boson- W -boson-neutral Higgs boson interaction is given by

$$\mathcal{L}_{WWH^0} = \sum_{r=1}^3 C^{WWH_r^0} H_r^0 W_\mu^+ W^{-\mu}. \quad (10)$$

The expression for the coefficient is

$$C^{WWH_r^0} = g m_W [O_{r1} \cos \beta + O_{r2} \sin \beta], \quad (11)$$

where m_W is a mass of the W -boson. Numerically, the magnitude of $C^{WWH_r^0}$ is the largest for the lightest Higgs H_2^0 , and the others are much smaller as we explicitly see in Section VI.

The chargino-neutralino- W -boson interactions are given by

$$\mathcal{L}_{\chi\chi^\pm W^\mp} = \sum_{k=1}^2 \overline{\chi}_k^- \gamma^\mu \left(C_L^{\chi_k^+ \chi W^-} P_L + C_R^{\chi_k^+ \chi W^-} P_R \right) \chi W_\mu^- + \text{h.c.}, \quad (12)$$

where $P_L = (1 - \gamma_5)/2$, $P_R = (1 + \gamma_5)/2$ and

$$\begin{aligned} C_L^{\chi_k^+ \chi W^-} &= -g \left(\sqrt{\frac{1}{2}} N_{13}^* U_{k2} + N_{12}^* U_{k1} \right), \\ C_R^{\chi_k^+ \chi W^-} &= g \left(\sqrt{\frac{1}{2}} N_{14} V_{k2}^* - N_{12} V_{k1}^* \right). \end{aligned} \quad (13)$$

The 2×2 unitary matrices U and V diagonalize the chargino mass matrix \mathcal{M}_{χ^-} as $U^* \mathcal{M}_{\chi^-} V^{-1} = \operatorname{diag}(m_{\chi_1^-}, m_{\chi_2^-})$ [18]. Note that these couplings are vanishing in a pure bino limit.

Finally, trilinear couplings for the neutral Higgs fields are given by

$$\mathcal{L}_{H^0 H^0 H^0} = \sum_{r,s,t=1}^3 \frac{1}{3!} C^{H_r^0 H_s^0 H_t^0} H_r^0 H_s^0 H_t^0. \quad (14)$$

The coupling constant $C^{H_r^0 H_s^0 H_t^0}$ is written as

$$C^{H_r^0 H_s^0 H_t^0} = \frac{gm_Z}{4 \cos \theta_W} \left[(O_{r1} \cos \beta - O_{r2} \sin \beta)(O_{s2} O_{t2} - O_{s1} O_{t1} + O_{s3} O_{t3} \cos 2\beta) \right. \\ \left. + (\text{the other permutations of } r, s, t) \right], \quad (15)$$

where m_Z is the Z -boson mass, and θ_W denotes the Weinberg angle.

III. NEUTRALINO PAIR ANNIHILATIONS WITH CP VIOLATION

Neutralino pair annihilations are of importance when we examine the relic density of the neutralino and its indirect detection. The complete expressions for the total cross section of neutralino pair annihilations in the case of no CP violation are found in Ref. [18]. We have extended the analysis of Ref. [18] to incorporate the effects of CP violation, and derived the full expressions for the neutralino annihilation cross section at the tree level with CP-violating phases, taking into account the modified interactions including (7), (10) and (12). Calculation of the total pair annihilation cross section σ involves a number of final states:

$$\chi\chi \longrightarrow f\bar{f}, H_r^0 H_s^0 (r, s = 1, 2, 3), H^+ H^-, \\ W^+ W^-, ZZ, W^\pm H^\mp, ZH_r^0 (r = 1, 2, 3). \quad (16)$$

The complete set of the analytic expressions including all the final states are quite lengthy and complicated, so we do not list the full result. Instead, we present only some of the results for the W -boson pair production $\chi\chi \rightarrow W^+ W^-$ and the lightest Higgs boson pair production $\chi\chi \rightarrow H_2^0 H_2^0$ which are essential in later discussion. In our numerical analysis in section VI, however, we include all the contributions to

the neutralino annihilation cross section at the tree level. Note that we can assume nonrelativistic neutralinos in the analysis of positron flux, while we have to keep the exact form to calculate the relic density.

Before presenting the expressions with CP violation, let us briefly summarize some generic features on the cross sections in the case without CP violation. When the LSP is bino-like, the fermion pair production $\chi\chi \rightarrow f\bar{f}$ ($f = u, c, t, \dots$) typically gives a dominant contribution to the total pair annihilation cross section for nonrelativistic neutralinos. There are three diagrams which contribute to this process: neutral Higgs boson exchange, Z -boson exchange and sfermion exchange (see Fig. 1). The s-wave amplitude of this process for nonrelativistic neutralinos is always suppressed by a fermion mass (except for the top quark). Because of the s-wave suppression, the cross section of a light fermion pair production from nonrelativistic neutralino annihilations is much smaller than that for a heavy fermion. If the neutralino is heavier than the W -boson and/or the lightest Higgs boson, the processes $\chi\chi \rightarrow W^+W^-$ and/or $\chi\chi \rightarrow H_2^0 H_2^0$ open up. However, for a bino-like LSP, these processes give smaller contributions than that for the $f\bar{f}$ final state in the case without CP violation.

On the other hand, when the LSP is higgsino-like, the W -boson pair production $\chi\chi \rightarrow W^+W^-$ gives a dominant contribution if the neutralino is heavy enough. This process involves three diagrams: neutral Higgs boson exchange, Z -boson exchange and chargino exchange (see Fig. 2). Since this contribution has no s-wave suppression, the neutralino pair annihilation cross section is much enhanced so that the resultant relic density of the neutralino is typically too small to satisfy the WMAP constraint (1).

However, in the presence of CP violation, new features appear in the W -boson pair production for a bino-like LSP. In order to see this fact, let us present essential parts of the analytic results for the cross section of $\chi\chi \rightarrow W^+W^-$ in the following.

The analytic expression for the neutral Higgs exchange contribution to $\chi\chi \rightarrow WW$ is given by

$$\sigma_{WW}^{(H)} v = \frac{\beta_W}{32\pi m_\chi^2} \frac{s^2 - 4m_W^2 s + 12m_W^4}{8m_W^4}$$

$$\times \left[(s - 4m_\chi^2) \left| \sum_{r=1}^3 \frac{C^{WWH_r^0} C_S^{\chi\chi H_r^0}}{P_{H_r^0}(s)} \right|^2 + s \left| \sum_{r=1}^3 \frac{C^{WWH_r^0} C_P^{\chi\chi H_r^0}}{P_{H_r^0}(s)} \right|^2 \right], \quad (17)$$

where

$$P_{H_r^0}(s) = s - m_{H_r^0}^2 + i \Gamma_{H_r^0} m_{H_r^0}, \quad (18)$$

m_χ is a mass of the lightest neutralino, $\Gamma_{H_r^0}$ denotes the decay width of H_r^0 , $\beta_W = \sqrt{1 - 4m_W^2/s}$ is the velocity of the W -boson in the center of mass frame, and s is a Mandelstam variable. The relative velocity between the two colliding neutralinos is denoted by v . Numerically, the contribution from the lightest Higgs exchange ($r = 2$) is dominant as expected from eq. (11). Note that $C_P^{\chi\chi H_2^0}$ becomes nonzero in the presence of CP violation. For nonrelativistic neutralinos $s \rightarrow 4m_\chi^2$, the first term in the square bracket of eq. (17) vanishes. On the other hand, the second term includes the factor s rather than $s - 4m_\chi^2$. Therefore this term does not vanish in the nonrelativistic limit once CP violation is turned on.

Similarly, the chargino exchange contribution and the interference term between the Higgs and the chargino exchange diagrams for $\chi\chi \rightarrow W^+W^-$ contain contributions which do not vanish for $s \rightarrow 4m_\chi^2$ in the presence of CP violation. There are also other contributions to the W -boson pair production which include Z -boson exchange and possible interference terms, but we neglect them for the moment since they are typically subdominant. With all the relevant contributions together, the expression for the total cross section of $\chi\chi \rightarrow W^+W^-$ for nonrelativistic neutralinos ($v \rightarrow 0$) is given by

$$\begin{aligned} \sigma_{WW} v \Big|_{v \rightarrow 0} = & \frac{\beta_W}{8\pi} \left[(m_\chi^2 - m_W^2) \left| \sum_{k=1}^2 \frac{2C_{+k}^W}{\Delta_k^W} \right|^2 \right. \\ & \left. + \frac{4m_\chi^4 - 4m_W^2 m_\chi^2 + 3m_W^4}{2m_W^4} \left| \sum_{r=1}^3 \frac{C^{WWH_r^0} C_P^{\chi\chi H_r^0}}{P_{H_r^0}(4m_\chi^2)} - \sum_{k=1}^2 \frac{2D_{-k}^W m_{\chi_k^-}}{\Delta_k^W} \right|^2 \right], \end{aligned} \quad (19)$$

where $\Delta_k^W = m_W^2 - m_\chi^2 - m_{\chi_k^-}^2$ and

$$\begin{aligned} C_{+k}^W &= \frac{1}{2} \left[\left| C_L^{\chi_k^+ \chi W^-} \right|^2 + \left| C_R^{\chi_k^+ \chi W^-} \right|^2 \right], \\ D_{-k}^W &= i \operatorname{Im} \left[C_R^{\chi_k^+ \chi W^-} \left(C_L^{\chi_k^+ \chi W^-} \right)^* \right]. \end{aligned} \quad (20)$$

In eq. (19), the second term in the square bracket represents the effect of CP violation, while the first term does not vanish even without CP violation. Note that we include Z -boson exchange and possible interference terms in the numerical analysis even though we neglected them in eq. (19).

Likewise, the lightest Higgs boson pair production $\chi\chi \rightarrow H_2^0 H_2^0$ involves contributions which are drastically enhanced by CP violation. This process occurs via two diagrams: neutral Higgs boson exchange and neutralino exchange (see Fig. 3). The expression for the total cross section of this process for nonrelativistic neutralinos ($v \rightarrow 0$) is given by

$$\sigma_{H_2^0 H_2^0 v} \Big|_{v \rightarrow 0} = \frac{\beta_{H_2^0}}{16\pi} \left| \sum_{r=1}^3 \frac{C^{H_2^0 H_2^0 H_r^0} C_P^{\chi\chi H_r^0}}{P_{H_r^0}(4m_\chi^2)} - \sum_{i=1}^4 \frac{2D_{-i}^{H_2^0} m_{\chi_i^0}}{\Delta_i^{H_2^0}} \right|^2, \quad (21)$$

where $\Delta_i^{H_2^0} = m_{H_2^0}^2 - m_\chi^2 - m_{\chi_i^0}^2$, $\beta_{H_2^0}$ denotes the velocity of H_2^0 in the center of mass frame, $m_{\chi_i^0}$ is the mass of the neutralino χ_i^0 , and

$$D_{-i}^{H_2^0} = 2i \operatorname{Im} \left[C_S^{\chi_i^0 \chi H_2^0} \left(C_P^{\chi_i^0 \chi H_2^0} \right)^* \right]. \quad (22)$$

Note that the cross section (21) is vanishing in the absence of CP violation.

The above expressions (19) and (21) are valid only for the nonrelativistic limit $s \rightarrow 4m_\chi^2$. In our numerical calculation, however, we use the exact expression for general s instead of the above expressions.

IV. RELIC DENSITY OF THE NEUTRALINO

In this section, we briefly review the formalism to compute the neutralino relic density in the MSSM with supersymmetric CP violation [5]. The time evolution

of the neutralino number density n_χ in the expanding Universe is described by the Boltzmann equation

$$\frac{dn_\chi}{dt} + 3Hn_\chi = -\langle\sigma v\rangle [n_\chi^2 - (n_\chi^{\text{eq}})^2], \quad (23)$$

where H is the Hubble expansion rate, n_χ^{eq} is the number density which the neutralino would have in thermal equilibrium, and σ is the total cross section of the neutralino pair annihilation into ordinary particles. The quantity $\langle\sigma v\rangle$ represents a thermal average of σv .

In the early Universe, the neutralino is assumed to be in thermal equilibrium where $n_\chi = n_\chi^{\text{eq}}$. As the Universe expands, the neutralino annihilation process freezes out, and after that the number of the neutralinos in a comoving volume remains constant. Using an approximate solution to eq. (23), the relic energy density $\rho_\chi = m_\chi n_\chi$ at present is given by

$$\rho_\chi = \sqrt{\frac{4\pi^3 g_* G_N}{45}} \left(\frac{T_\chi}{T_\gamma}\right)^3 T_\gamma^3 \frac{1}{\int_0^{x_F} dx \langle\sigma v\rangle}, \quad (24)$$

where $x = T/m_\chi$ is a temperature of the neutralino normalized by its mass, g_* (≈ 81) represents the effective number of degrees of freedom at freeze-out, and G_N denotes the Newton's constant. T_χ and T_γ are the present temperatures of the neutralino and the photon, respectively. The suppression factor $(T_\chi/T_\gamma)^3 \approx 1/20$ follows from the entropy conservation in a comoving volume [34]. The value of x at freeze-out, x_F , is obtained by solving the following equation iteratively:

$$x_F^{-1} = \ln \left(\frac{m_\chi}{2\pi^3} \sqrt{\frac{45}{2g_* G_N}} \langle\sigma v\rangle_{x_F} x_F^{1/2} \right). \quad (25)$$

Typically one finds $x_F \approx 1/20$ which implies that the neutralinos are nonrelativistic at freeze-out.

The thermal average in eq. (23) should be carefully treated for accurate calculation of the relic density. In literatures, expansion of the thermal average in powers of the temperature $\langle\sigma v\rangle \approx a + bx$ is widely used. However, it is known that the expansion

breaks down when σ varies rapidly with the energy of the neutralinos, hence, in general, one has to use the exact expression for the thermal average [13]

$$\langle\sigma v\rangle = \frac{1}{8m_\chi^4 T K_2^2(m_\chi/T)} \int_{4m_\chi^2}^{\infty} ds \sigma(s)(s - 4m_\chi^2) \sqrt{s} K_1\left(\frac{\sqrt{s}}{T}\right), \quad (26)$$

where K_i ($i = 1, 2$) are the modified Bessel functions. Note that we should not take the nonrelativistic limit $v \rightarrow 0$ to calculate the cross section σ in the integrand. In our analysis, we perform a numerical evaluation of the exact thermal average (26) to obtain the relic density accurately.

In the present analyses, we neglect coannihilation effects [35, 36, 37, 38, 39, 40, 41], although they are crucial when the next-lightest superparticle is nearly degenerated with the LSP. The investigation of the effect of CP violation on the coannihilation cross sections is left for future work.

V. POSITRONS FROM NEUTRALINO ANNIHILATIONS IN THE GALACTIC HALO

Cosmic ray observations provide interesting probes for indirect detection of CDM. Even though the neutralino pair annihilations described in section IV have already frozen out at present, neutralinos gravitationally accumulated in the galactic halo still can pair-annihilate to produce, e.g., cosmic γ -rays, neutrinos, antiprotons and positrons [5, 6]. Among various such observations, the High-Energy Antimatter Telescope (HEAT) reported an excess of cosmic ray positrons [42]. Previous analyses on the positron flux in the MSSM without CP violation have suggested that some enhancement mechanism such as nontrivial distribution of CDM and/or so-called boost factors is necessary in order to explain the excess by neutralino LSP annihilations [43, 44, 45].

We describe our procedure to evaluate the positron flux from neutralino pair annihilations in the galactic halo in the following. The positron flux we measure can be

written as [43, 44]

$$\frac{dF_+}{dE} = \frac{\rho_0^2}{m_\chi^2} \int d\epsilon G(E, \epsilon) \sum_i (\sigma_i v) f_i(\epsilon), \quad (27)$$

where $v = 10^{-3}$ is a typical neutralino velocity in the galactic halo, and $\rho_0 = 0.43$ GeV/cm³ represents a local halo dark matter density. Positrons produced in the halo are decelerated or accelerated during propagation in the halo until they are detected. The energy of a positron at detection is denoted by E , while that at production is denoted by ϵ . The function $G(E, \epsilon)$ is a Green's function which describes propagation of positrons in the galactic halo. In our calculation, we use the Green's function in Ref. [43] with a containment time $\tau = 10^7$ yr. The cross section σ_i represents that for the process $\chi\chi \rightarrow i$, where the symbol i runs over every possible final state: $i = f\bar{f}$, W^+W^- , etc. Computation of the positron flux requires the cross sections σ_i only for $v = 10^{-3}$. In our numerical calculation of σ_i for $v = 10^{-3}$, we use $s \approx 4m_\chi^2(1 + v^2)$.

The function $f_i(\epsilon)$ is the positron energy spectrum at production which originates from the process $\chi\chi \rightarrow i$. There are many contributions to $f_i(\epsilon)$, and some of them including hadronization are not calculable. In order to perform a detailed analysis, one has to utilize a Monte Carlo simulation code such as PYTHIA [46]. In the present analysis, however, we content ourselves with a rough estimation to calculate $f_i(\epsilon)$, employing the methods used in Refs. [43, 44] as follows.

The most energetic positron comes from the direct production $\chi\chi \rightarrow e^+e^-$ where the positron has the maximal energy $\epsilon \approx m_\chi$. However the cross section is extremely small due to the s-wave suppression by the electron mass so that this contribution is invisible. On the other hand, heavy fermion productions $\chi\chi \rightarrow c\bar{c}$, $b\bar{b}$, $\tau^+\tau^-$ and $t\bar{t}$, may produce enough positrons as decay products (e.g., $\bar{b} \rightarrow \bar{c}W^{+*}$ followed by $W^{+*} \rightarrow e^+\nu_e$), where the typical positron energy is $\epsilon \approx m_\chi/3$. Also, hadronization of quarks results in a shower of charged pions, and the contribution of the positrons from charged pion decay ($\pi^+ \rightarrow \mu^+ \rightarrow e^+$) are evaluated using the data from e^+e^- collider experiments as in Ref. [44].

For a neutralino heavier than the W -boson, positrons with energy $\epsilon \approx m_\chi/2$ can

be produced by the W -boson production $\chi\chi \rightarrow W^+W^-$ followed by the decay $W^+ \rightarrow e^+\nu_e$. There is also continuum positron radiation from muons, τ -leptons and heavy quarks produced in the W -boson decay (i.e., $W^+ \rightarrow \mu^+ \rightarrow e^+$, $W^+ \rightarrow \tau^+ \rightarrow e^+$, etc.). The contribution of positrons from decay of charged pions produced in the W -boson pair production is estimated as in Ref. [43]. Similarly, contributions from the Z -boson pair production $\chi\chi \rightarrow ZZ$ followed by the decays $Z \rightarrow e^+e^-$, etc. are also included. It is known that, when the LSP is higgsino-like, the gauge boson final states W^+W^- and ZZ can give rise to enough positron excess [43]. For the process including H_2^0 in the final state, positrons from $H_2^0 \rightarrow b\bar{b}$ are taken into account.

For the cosmic ray electron flux, we use $\frac{dF_-}{dE} = 0.07 (E/\text{GeV})^{-3.3} \text{ cm}^{-2}\text{sr}^{-1}\text{GeV}^{-1}\text{sec}^{-1}$ [47]. The background flux of cosmic ray positrons are estimated with $\frac{dF_+/dE}{dF_+/dE + dF_-/dE} = 0.02 + 0.10(E/\text{GeV})^{-0.5}$ [48].

VI. NUMERICAL RESULTS

In this section, we present our numerical results. In all the figures, we fix some of the parameters in eq. (3) as

$$m_0 = |A| = 1 \text{ TeV}, \quad m_A = 500 \text{ GeV}, \quad \tan\beta = 5, \quad (28)$$

and consider variations of the remaining parameters as follows

$$\begin{aligned} \theta_\mu &= 0 - \pi, \quad \theta_A = 0 - \pi, \\ M_2 &= 100 - 700 \text{ GeV}, \quad |\mu| = 100 - 700 \text{ GeV}. \end{aligned} \quad (29)$$

In what follows, we shall show that the process $\chi\chi \rightarrow W^+W^-$ or $\chi\chi \rightarrow H_2^0 H_2^0$ can give a significant contribution to σv in the presence of CP violation. For this purpose, let us first present the magnitude of the relevant couplings in this process.

We begin with a discussion of the t- and u-channel chargino exchange diagram (see Fig. 2) which is known to give a dominant contribution to $\chi\chi \rightarrow W^+W^-$ in the absence of CP violation. In Fig. 4, the quantities C_{+1}^W and D_{-1}^W defined in eq. (20)

involved in the lighter chargino exchange contribution to $\chi\chi \rightarrow W^+W^-$ are plotted as a function of the CP violating phase θ_μ for $M_2 = 300$ GeV, $|\mu| = 400$ GeV and $\theta_A = 0$ with the other parameters fixed as in eq. (28). The dashed and solid curves correspond to the result for C_{+1}^W and D_{-1}^W , respectively. It is seen that both C_{+1}^W and D_{-1}^W have nontrivial dependence on θ_μ . The magnitudes of the coefficients in eq. (2) for this choice of parameters are obtained as $|N_{11}|^2 \approx 0.97$, $|N_{12}|^2 \lesssim 0.003$, $|N_{13}|^2 \lesssim 0.02$ and $|N_{14}|^2 \lesssim 0.006$, hence the LSP is bino-like. Of course, the Higgs exchange diagram is absent if χ is a pure bino. However, χ actually has small but nonvanishing higgsino components due to bino–higgsino mixings even when M_1 is much smaller than $|\mu|$. The small higgsino components turn out to play a crucial role in the calculation of neutralino pair annihilation cross sections.

In the presence of CP violation, the largest contribution to $\chi\chi \rightarrow W^+W^-$ can be given by the neutral Higgs exchange diagram which includes three coupling constants $C^{WWH_r^0}$, $C_P^{\chi\chi H_r^0}$ and $C_S^{\chi\chi H_r^0}$ ($r = 1, 2, 3$). In Fig. 5, the dependence of the absolute value of the coupling constants $C^{WWH_r^0}$ on θ_μ is presented for the same choice of parameters as Fig. 4. It is seen that the coupling $C^{WWH_r^0}$ is the largest for the lightest Higgs H_2^0 independent of θ_μ .

On the other hand, the imaginary parts of the pure imaginary coupling constants $C_P^{\chi\chi H_r^0}$ ($r = 1, 2, 3$) for the same choice of parameters are shown in Fig. 6. Without CP violation, only the coupling for H_3^0 is nonvanishing. In the presence of CP violation, however, the couplings for H_1^0 and H_2^0 also become nonvanishing and even comparable to that for H_3^0 . As these figures clearly show, the lightest Higgs exchange diagram gives the dominant contribution among the three Higgs exchange contributions. We do not show a result for the coupling $C_S^{\chi\chi H_r^0}$, since it is not essential for our discussion.

In Fig. 7, the cross section times relative velocity σv for $v = 10^{-3}$ is shown for the same choice of parameters as Fig. 4. The solid, long dash-dot, short dashed, short dash-dot and short dash-long dash lines correspond to the contributions from W^+W^- , ZZ , $b\bar{b}$, $\tau^+\tau^-$ and $H_2^0H_2^0$ final states, respectively. The bold solid line represents the sum of all the contributions. Without CP violation ($\theta_\mu = 0, \pi$), a fermionic final state,

$b\bar{b}$, is dominant as usually expected for a bino-like LSP. In this case, the cross section of $\chi\chi \rightarrow W^+W^-$ is dominated by the chargino exchange diagram in Fig. 2 and the Higgs and Z -boson exchange contributions are negligible. The resultant contribution of the W^+W^- final state is, however, smaller than the $b\bar{b}$ contribution. For $\theta_\mu \approx \pi/2$, the lightest Higgs exchange contribution to the W^+W^- production is much enhanced due to the effect of CP violation to dominate over the chargino exchange contribution. Because of this enhancement, the W^+W^- contribution can be larger than the $b\bar{b}$ contribution. Similar enhancement due to CP violation can be seen for ZZ and $H_2^0 H_2^0$ final states. It is found that the W^+W^- or $H_2^0 H_2^0$ final state gives the largest contribution for $0.1\pi \lesssim \theta_\mu \lesssim 0.9\pi$.

In Fig. 8, the relic density $\Omega_\chi h^2$ is shown as a function of θ_μ for the same choice of parameters as Fig. 4. In the shaded region, the relic density is consistent with the 2σ allowed range of the WMAP result

$$0.094 < \Omega_\chi h^2 < 0.129. \quad (30)$$

It is found that the relic density is considerably suppressed for $\theta_\mu \approx \pi/2$. However, the relic density is still too large to satisfy the WMAP constraint even for $\theta_\mu \approx \pi/2$. In the presence of CP violation, the cross section is certainly much enhanced, but even this enhancement can not make bino-like dark matter consistent with the cosmological constraint. In order to make the bino-like LSP cosmologically allowed, one has to resort to some other mechanism such as resonant annihilations or coannihilations by tuning some parameter.

The θ_A dependence of σv for $v = 10^{-3}$ is shown in Fig. 9 for the same choice of parameters as Fig. 4 but $\theta_\mu = 0$. It is seen that all the relevant contributions are insensitive to θ_A . As a result, the relic density is also insensitive to θ_A ($\Omega_\chi h^2 \approx 3.3$). We have not found any significant dependence on θ_A even if we vary M_2 and μ for our choice of the other parameters in eq. (28).

When the higgsino components are increased, the relic density shows different behavior. Fig. 10 represents the θ_μ dependence of σv for $v = 10^{-3}$ in the case of

$M_2 = 300 \text{ GeV}$ and $|\mu| = 200 \text{ GeV}$ where the LSP has sizable higgsino components. The values of the other parameters are the same as Fig. 4. The magnitudes of the coefficients in eq. (2) for this choice of parameters are obtained as $|N_{11}|^2 \approx 0.65$, $|N_{12}|^2 \lesssim 0.03$, $|N_{13}|^2 \approx 0.2$ and $|N_{14}|^2 \approx 0.1$, hence the LSP can be regarded as a mixture of the bino and the higgsinos. For such a mixed LSP, the magnitude of the couplings $C_L^{\chi_1^+ \chi W^-}$ and $C_R^{\chi_1^+ \chi W^-}$ in eq. (13) are increased compared with the case of a bino-like LSP. Because of this enhancement, the W^+W^- final state gives a dominant contribution $\sigma v \approx 10^{-9} \text{ GeV}^{-2}$ for any θ_μ . The ZZ and $H_2^0 H_2^0$ final states are also much enhanced and either of them gives the second largest contribution. However, the cross sections for the gauge boson final states W^+W^- and ZZ are less sensitive to θ_μ for a mixed LSP than the case of a bino-like LSP, even though the $H_2^0 H_2^0$ final state still has an enhancement for $\theta_\mu \approx \pi/2$. Therefore, the total cross section shows only mild dependence on θ_μ . One might expect that the W^+W^- final state is also enhanced as in the case for the $H_2^0 H_2^0$ final state. However, what actually happens is that there occurs a considerable cancellation between the Higgs exchange and the chargino exchange diagrams for a mixed LSP². Because of this cancellation, the W^+W^- final state shows only mild dependence on θ_μ . Similar cancellation occurs for the ZZ final state as well.

The relic density for the same choice of parameters as Fig. 10 is shown in Fig. 11. For a mixed LSP, the θ_μ dependence of $\Omega_\chi h^2$ is much weaker than the case of a bino-like LSP. However, it is found that the allowed region appear at $\theta_\mu \approx 2\pi/3$. Thus CP violation can be essential to find cosmologically allowed regions in the parameter space.

Let us briefly comment on a higgsino-like LSP. When χ is higgsino-like, the couplings $C_L^{\chi_1^+ \chi W^-}$ and $C_R^{\chi_1^+ \chi W^-}$ in eq. (13) have a maximal magnitude of order g without any other small suppression factor, and almost insensitive to θ_μ . In this case, the W^-

² In the first version of this paper, the sign of the interference term between the Higgs exchange and the chargino exchange diagrams in the process $\chi\chi \rightarrow W^+W^-$ was wrong. Hence this cancellation was not seen in the first version.

boson pair production gives the dominant contribution, and this leads to a much larger cross section $\sigma v \approx 10^{-8} \text{ GeV}^{-2}$ than that for a bino-like or a mixed LSP. Therefore the relic density for a higgsino-like LSP is too small to satisfy the WMAP constraint, and almost insensitive to θ_μ .

Let us present a global map in the $(|\mu|, M_2)$ plane. In Fig. 12, the final states giving the largest contribution to σv for $v = 10^{-3}$ are displayed in the $(|\mu|, M_2)$ plane for $m_0 = |A| = 1 \text{ TeV}$, $m_A = 500 \text{ GeV}$, $\tan\beta = 5$, $\theta_A = 0$ and $\theta_\mu = 0$. The regions where the final states W^+W^- , $b\bar{b}$, $t\bar{t}$ and $W^\pm H^\mp$ give the largest contribution are shown in different gray scales. The white region is excluded by the LEP limit on the chargino mass $m_{\chi_1^\pm} > 104 \text{ GeV}$ [49] and the lightest Higgs mass $m_{H_2^0} > 113 \text{ GeV}$ [50]. For a bino-like LSP ($M_2 \ll |\mu|$), the $b\bar{b}$ final state typically gives the largest contribution, while for a higgsino-like LSP ($M_2 \gg |\mu|$), the W^+W^- final state is the largest. When the LSP is relatively heavy, the $t\bar{t}$ final state can be the largest. When both M_2 and $|\mu|$ are large ($\approx 700 \text{ GeV}$), the $W^\pm H^\mp$ final state is the largest. In the darkest strip in Fig. 12, the relic density is consistent with the WMAP 2σ constraint. In the region $M_2 \approx 500 \text{ GeV}$, where $2m_\chi \approx m_{H_3^0}$, there occurs resonant annihilation to the $b\bar{b}$ and $t\bar{t}$ final states via heavy Higgs boson exchange, so that the WMAP allowed region is extended to a large $|\mu|$ region for $M_2 \approx 500 \text{ GeV}$. It is seen that aside from the resonant annihilation region, the cosmological constraint (30) is satisfied for a mixed LSP. For a bino-like LSP, the relic density is too large to satisfy the cosmological constraint (30), while it is too small for a higgsino-like LSP.

The similar result to Fig. 12 but for $\theta_\mu = \pi/2$ is shown in Fig. 13. It is found that, unlike the case without CP violation, the W^+W^- production is significantly enhanced and gives the largest contribution even for a bino-like LSP. Note, however, that even this enhancement of the W^+W^- final state can not save the bino-like region, as the WMAP allowed region does not appear for $M_2 < |\mu|$ except for the resonant annihilation region in Fig. 13. Also, there appears a region where the $H_2^0 H_2^0$ final state gives the largest contribution.

In Fig. 14, variation of the relic density with θ_μ normalized by that for $\theta_\mu = 0$,

$\Omega_\chi(\theta_\mu)/\Omega_\chi(\theta_\mu = 0)$, is shown as a function of M_2 for $m_0 = |A| = 1$ TeV, $m_A = 500$ GeV, $\tan\beta = 5$ and $\theta_A = 0$. Varying θ_μ in the range $0 < \theta_\mu < \pi$, the relic density lies between the two solid lines for $|\mu| = 200$ GeV. The region between the two dashed lines represents the corresponding result for $|\mu| = 600$ GeV. It is confirmed from this figure that the variation of the relic density with θ_μ is typically small for a higgsino-like LSP.

Finally we illustrate the effect of CP violation on the positron flux from neutralino annihilations in the galactic halo. The positron fraction $e^+/(e^+ + e^-)$ versus positron energy E_{e^+} is shown in Fig. 15 for the same choice of parameters as in Fig. 10. The LSP in this case is a mixture of the bino and the higgsinos. The dashed and solid lines correspond to the results for $\theta_\mu = 0$ and $\theta_\mu = \pi/2$, respectively. The points with error bars represent the data from HEAT measurement [42]. For both $\theta_\mu = 0$ and $\theta_\mu = \pi/2$, the positron flux is dominated by the background so that the supersymmetric contribution from the LSP annihilations is almost invisible. The similar result for $M_2 = 600$ GeV with the other parameters fixed as in Fig. 15. is shown in Fig. 16. This choice of parameters corresponds to a higgsino-like LSP. In this case, the supersymmetric contribution gives a large excess due to enhancement of the cross sections for the W^+W^- and ZZ final states, as generically expected for a higgsino-like LSP [43]. However, it is difficult to see the effect of CP violation, since the deviation of the solid line from the dashed one is very small in Fig. 16. In the case of a bino-like LSP as in Fig. 4, the neutralino pair annihilation cross section is smaller than that for the case of a mixed LSP. Therefore the supersymmetric contribution to the positron flux is completely invisible.

In the present analysis, we have not included coannihilation effects [35, 36, 37, 38, 39, 40, 41] in the calculation of the relic density. They are crucial in the case that the next-lightest superparticle is nearly degenerated with the LSP. Since this situation happens when the LSP is higgsino-like, our results on the relic density for a higgsino-like LSP may be altered if coannihilations are taken into account. The investigation of the effect of CP violation on the coannihilations is left for future work.

VII. CONCLUSIONS

We have studied pair annihilations of the neutralino dark matter in the minimal supersymmetric standard model with CP violation. We have considered the case that the higgsino mass and the trilinear scalar couplings have CP-violating phases of order unity, taking a scenario that the scalar fermions in the first two generations are much heavier than those in the third generation to avoid a severe constraint from experimental limits on electric dipole moments. It has been found that, when the lightest neutralino is bino-like, the cross section of the process $\chi\chi \rightarrow W^+W^-$ and $\chi\chi \rightarrow H_2^0 H_2^0$ for nonrelativistic neutralinos can be significantly enhanced by θ_μ , the phase of the higgsino mass. It follows that the relic density of the neutralino can be considerably suppressed by this effect. However, even this enhancement is not enough to make bino-like dark matter consistent with the cosmological constraint (30). We have also discussed the effect of CP violation on the positron flux from neutralino pair annihilations in the galactic halo. It has been shown that the effect of CP violation is difficult to see in the positron flux.

Acknowledgments

The author was supported in part by the Grant-in-Aid for Scientific Research (No.16740150) from the Ministry of Education, Culture, Sports, Science and Technology of Japan. The author thanks G. Belanger, S. Kraml and S. Pukhov for pointing out the possible cancellation in the W -boson pair production with CP violation.

-
- [1] E. Kolb and M. Turner, *The Early Universe*, Addison-Wesley (1990).
 - [2] C.L. Bennett *et.al.*, *Astrophys. J. Suppl.* **148**, 1 (2003); D.N. Spergel *et.al.*, *Astrophys. J. Suppl.* **148**, 175 (2003).
 - [3] W. Freedman, *Phys. Rep.* **333**, 13 (2000).

- [4] J.A. Tauber *et.al.* (The Planck Collaboration), *Advances in Space Research* **34**, 491 (2004).
- [5] For reviews on supersymmetric dark matter, see for instance, G. Jungman, M. Kamionkowski and K. Griest, *Phys. Rep.* **267**, 195 (1996).
- [6] For recent comprehensive reviews on particle dark matter, see for instance, G. Bertone, D. Hooper and J. Silk, *Phys. Rep.* **405**, 279 (2005).
- [7] For reviews on the MSSM, see for instance, H.P. Nilles, *Phys. Rep.* **110**, 1 (1984); H.E. Haber and G.L. Kane, *Phys. Rep.* **117**, 75 (1985); J.F. Gunion and H.E. Haber, *Nucl. Phys.* **B 272**, 1 (1986).
- [8] H. Goldberg, *Phys. Rev. Lett.* **50**, 1419 (1983); J.R. Ellis, J.S. Hagelin, D.V. Nanopoulos, K.A. Olive and M. Srednicki, *Nucl. Phys.* **B 238**, 453 (1984).
- [9] M. Srednicki, R. Watkins and K.A. Olive, *Nucl. Phys.* **B 310**, 693 (1988).
- [10] J.R. Ellis, L. Roszkowski and Z. Lalak, *Phys. Lett.* **B 245**, 545 (1990); K.A. Olive and M. Srednicki, *Nucl. Phys.* **B 355**, 208 (1991).
- [11] M. Drees and M.M. Nojiri, *Phys. Rev.* **D 47**, 376 (1993).
- [12] K. Griest, M. Kamionkowski and M.S. Turner, *Phys. Rev.* **D 41**, 3565 (1990).
- [13] P. Gondolo and G. Gelmini, *Nucl. Phys.* **B 360**, 145 (1991).
- [14] J.L. Lopez, D.V. Nanopoulos and K. Yuan, *Phys. Rev.* **D 48**, 2766 (1993).
- [15] H. Baer and M. Brhlik, *Phys. Rev.* **D 53**, 597 (1996).
- [16] T. Nihei, L. Roszkowski and R. Ruiz de Austri, *J. High Energy Phys.* **0105**, 063 (2001).
- [17] L. Roszkowski, R. Ruiz de Austri and T. Nihei *J. High Energy Phys.* **0108**, 024 (2001).
- [18] T. Nihei, L. Roszkowski and R. Ruiz de Austri, *J. High Energy Phys.* **0203**, 031 (2002).
- [19] A. Birkedal-Hansen and B.D. Nelson, *Phys. Rev.* **D 67**, 095006 (2003); A.B. Lahanas, N.E. Mavromatos and D.V. Nanopoulos, *Int. J. Mod. Phys.* **D12**, 1529 (2003); H. Baer, C. Balazs, A. Belyaev and J. O’Farrill, *J. Cosmo. Astropart. Phys.* **0309**, 007 (2003); H. Baer and J. O’Farrill, *J. Cosmo. Astropart. Phys.* **0404**, 005 (2004); H. Baer, A. Belyaev, T. Krupovnickas and X. Tata, *J. High Energy Phys.* **0402**, 007 (2004); A. Masiero, S. Profumo, S.K. Vempati and C.E. Yaguna, *J. High Energy Phys.* **0403**, 046

- (2004); H. Baer, A. Belyaev, T. Krupovnickas and A. Mustafayev, *J. High Energy Phys.* **0406**, 044 (2004); G. Belanger, F. Boudjema, A. Cottrant, A. Pukhov and A. Semenov, *Nucl. Phys.* **B 706**, 411 (2005); H. Baer, A. Mustafayev, S. Profumo, A. Belyaev and X. Tata, *J. High Energy Phys.* **0507**, 065 (2005); R. Dermisek, S. Raby, L. Roszkowski and R. Ruiz De Austri, hep-ph/0507233.
- [20] A.G. Cohen, D.B. Kaplan and A.E. Nelson, *Ann. Rev. Nucl. Part. Sci.* **43**, 27 (1993).
- [21] I. Affleck and M. Dine, *Nucl. Phys.* **B 249**, 361 (1985).
- [22] P.G. Harris *et.al.*, *Phys. Rev. Lett.* **82**, 904 (1999).
- [23] B.C. Regan, E.D. Commins, C.J. Schmidt and D. DeMille, *Phys. Rev. Lett.* **88**, 071805 (2002).
- [24] M.V. Romalis, W.C. Griffith and E.N. Fortson, *Phys. Rev. Lett.* **86**, 2505 (2001).
- [25] T. Falk, K.A. Olive and M. Srednicki, *Phys. Lett.* **B 354**, 99 (1995).
- [26] P. Gondolo and K. Freese, *J. High Energy Phys.* **0207**, 052 (2002).
- [27] A. Pilaftsis, *Phys. Lett.* **B 435**, 88 (1998); *Phys. Rev.* **D 58**, 096010 (1998); A. Pilaftsis and C.E.M. Wagner, *Nucl. Phys.* **B 553**, 3 (1999); D.A. Demir, *Phys. Rev.* **D 60**, 055006 (1999); S.Y. Choi, M. Drees and J.S. Lee, *Phys. Lett.* **B 481**, 57 (2000).
- [28] M. Carena, J.R. Ellis, A. Pilaftsis and C.E.M. Wagner, *Nucl. Phys.* **B 568**, 92 (2000); T. Ibrahim and P. Nath, *Phys. Rev.* **D 63**, 035009 (2001); S.W. Ham, S.K. Oh, E.J. Yoo, C.M. Kim and D. Son, *Phys. Rev.* **D 68**, 055003 (2003).
- [29] M.E. Gomez, T. Ibrahim, P. Nath and S. Skadhauge, *Phys. Rev.* **D 70**, 035014 (2004); hep-ph/0506243.
- [30] M. Argyrou, A.B. Lahanas, D.V. Nanopoulos and V.C. Spanos, *Phys. Rev.* **D 70**, 095008 (2004).
- [31] C. Balazs, M. Carena, A. Menon, D.E. Morrissey and C.E.M. Wagner, *Phys. Rev.* **D 71**, 075002 (2005).
- [32] T. Nihei and M. Sasagawa, *Phys. Rev.* **D 70**, 055011 (2004).
- [33] R.Dermisek, S. Raby, L. Roszkowski and R. Ruiz De Austri, *J. High Energy Phys.* **0304**, 037 (2003); hep-ph/0507233.

- [34] K.A. Olive, D. Schramm and G. Steigman, *Nucl. Phys.* **B 180**, 497 (1981).
- [35] K. Griest and D. Seckel, *Phys. Rev.* **D 43**, 3191 (1991).
- [36] S. Mizuta and M. Yamaguchi, *Phys. Lett.* **B 298**, 120 (1993).
- [37] J. Edsjö and P. Gondolo, *Phys. Rev.* **D 56**, 1879 (1997).
- [38] J.R. Ellis, T. Falk and K.A. Olive, *Phys. Lett.* **B 444**, 367 (1998); J.R. Ellis, T. Falk, K.A. Olive and M. Srednicki, *Astropart. Phys.* **13**, 181 (2000).
- [39] J.R. Ellis, T. Falk and Y. Santoso, *Astropart. Phys.* **18**, 395 (2003).
- [40] T. Nihei, L. Roszkowski and R. Ruiz de Austri, *J. High Energy Phys.* **0207**, 024 (2002).
- [41] H. Baer, C. Balazs and A. Belyaev, *J. High Energy Phys.* **0203**, 042 (2002); V.A. Bednyakov, H.V. Klapdor-Kleingrothaus and V. Gronewold, *Phys. Rev.* **D 66**, 115005 (2002).
- [42] S.W. Barwick *et.al.* (HEAT Collaboration), *Astrophys. J.* **482**, L191 (1997).
- [43] M. Kamionkowski and M.S. Turner, *Phys. Rev.* **D 43**, 1774 (1991).
- [44] S. Rudaz and F.W. Stecker, *Astrophys. J.* **325**, 16 (1988).
- [45] G.L. Kane, L.-T. Wang and J.D. Wells, *Phys. Rev.* **D 65**, 057701 (2002); E.A. Baltz, J. Edsjö, K. Freese and P. Gondolo, *Phys. Rev.* **D 65**, 063511 (2002); G.L. Kane, L.-T. Wang and T.T. Wang, *Phys. Lett.* **B 536**, 263 (2002); D. Hooper, J.E. Taylor and J. Silk, *Phys. Rev.* **D 69**, 103509 (2004); K. Belotsky, D. Fargion, M. Khlopov and R.V. Konoplich, hep-ph/0411093.
- [46] T. Sjöstrand *et.al.*, *Comput. Phys. Commun* **135**, 238-259 (2001).
- [47] D. Mueller and K.-K. Tang, *Astrophys. J.* **312**, 183 (1987).
- [48] R.J. Protheroe, *Astrophys. J.* **254**, 391 (1982).
- [49] Joint LEP 2 SUSY Working Group, ALEPH, DELPHI, L3 and OPAL experiments, note LEPSUSYWG/01-03.1 (<http://lepsusy.web.cern.ch/lepsusy/Welcome.html>).
- [50] LEP Higgs Working Group for Higgs boson searches, ALEPH, DELPHI, L3 and OPAL Collaborations, *Phys. Lett.* **B 565**, 61 (2003).

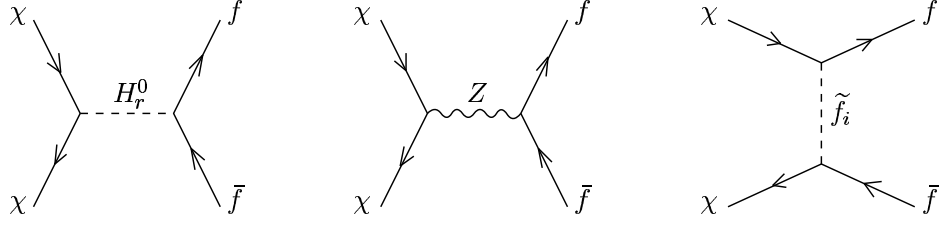


FIG. 1: Feynman diagrams for $\chi\chi \rightarrow f\bar{f}$: the s-channel neutral Higgs boson exchange, the s-channel Z -boson exchange, and the t- and u-channel sfermion exchange. Note that the u-channel diagram is not shown here.

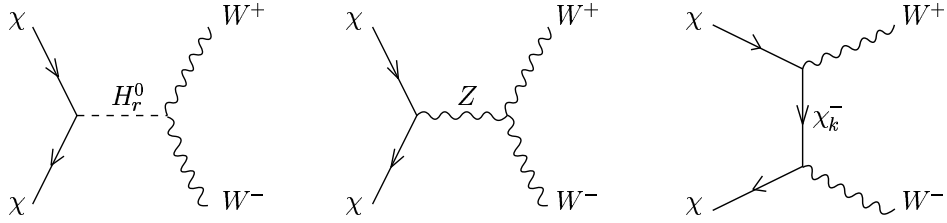


FIG. 2: Feynman diagrams for $\chi\chi \rightarrow W^+W^-$: the s-channel neutral Higgs boson exchange, the s-channel Z -boson exchange, and the t- and u-channel chargino exchange.

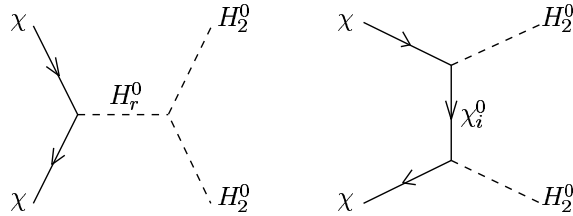


FIG. 3: Feynman diagrams for $\chi\chi \rightarrow H_2^0 H_2^0$: the s-channel neutral Higgs boson exchange and the t- and u-channel neutralino exchange.

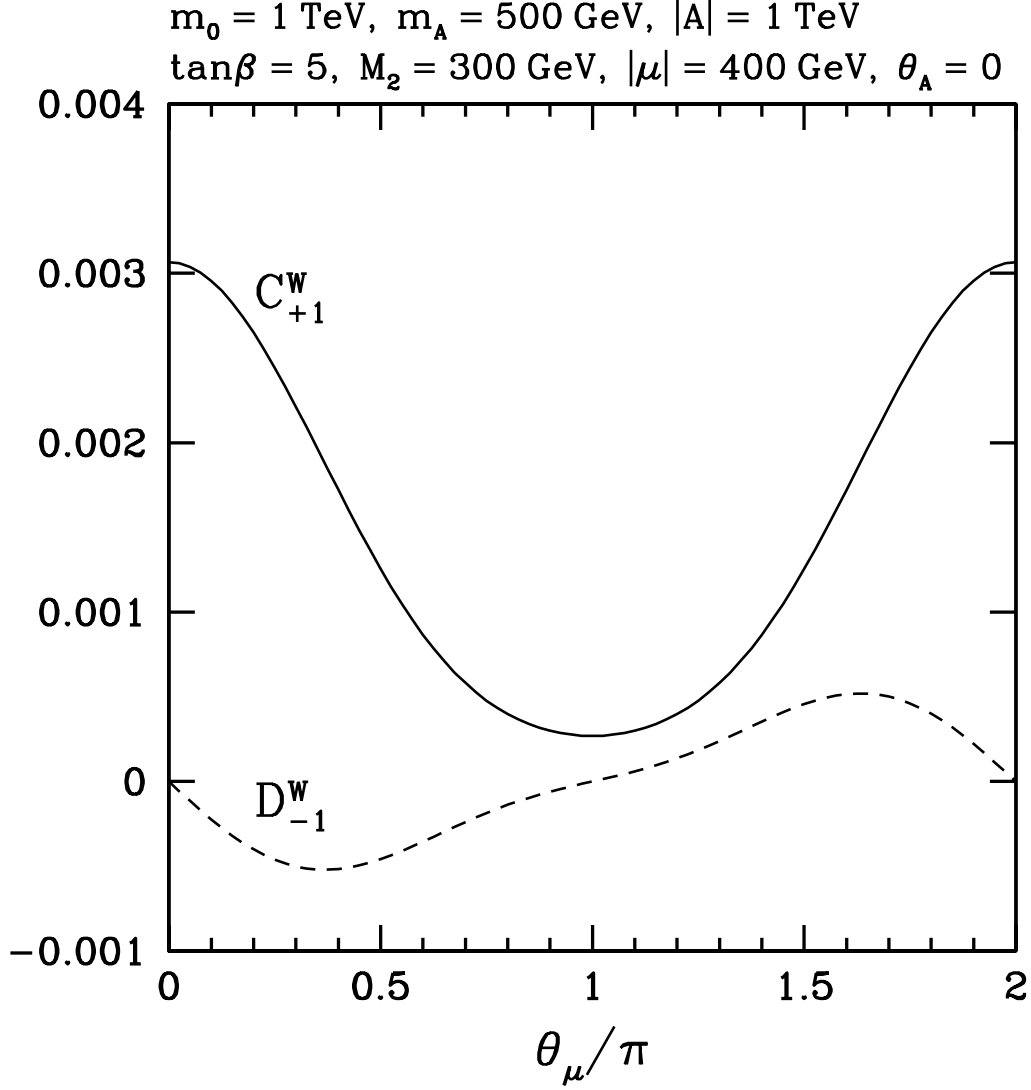


FIG. 4: The variation of the quantities C_{+1}^W and D_{-1}^W defined in eq. (20) with the CP violating phase θ_μ . The relevant parameters are taken as $m_0 = |A| = 1 \text{ TeV}$, $m_A = 500 \text{ GeV}$, $\tan\beta = 5$, $M_2 = 300 \text{ GeV}$, $|\mu| = 400 \text{ GeV}$ and $\theta_A = 0$. The dashed and solid curves correspond to the result for C_{+1}^W and D_{-1}^W , respectively. In this case, the LSP is bino-like.

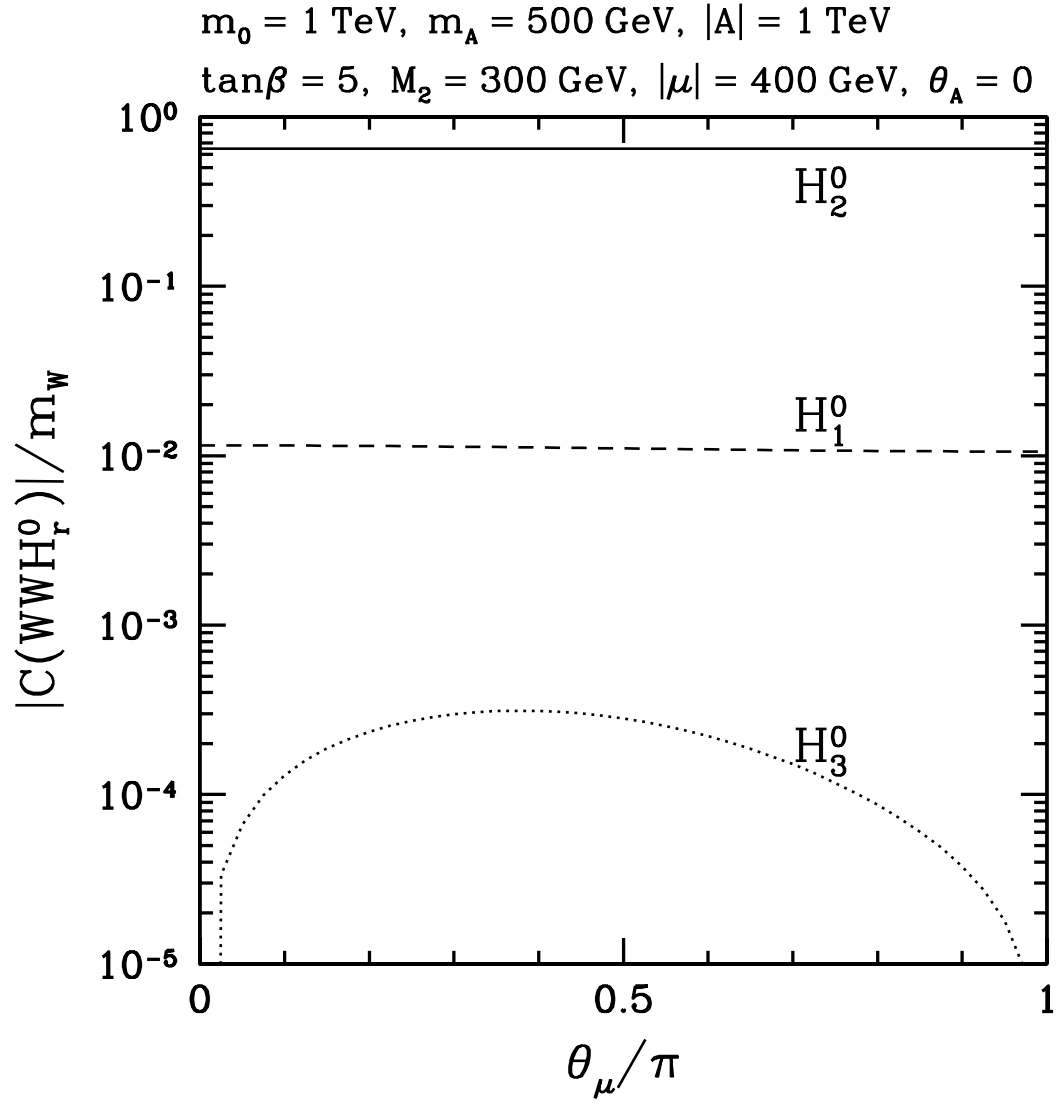


FIG. 5: The absolute value of the coupling constants $C^{WWH_r^0}$ ($r = 1, 2, 3$) normalized by m_W as a function of θ_μ for the same choice of parameters as Fig. 4.

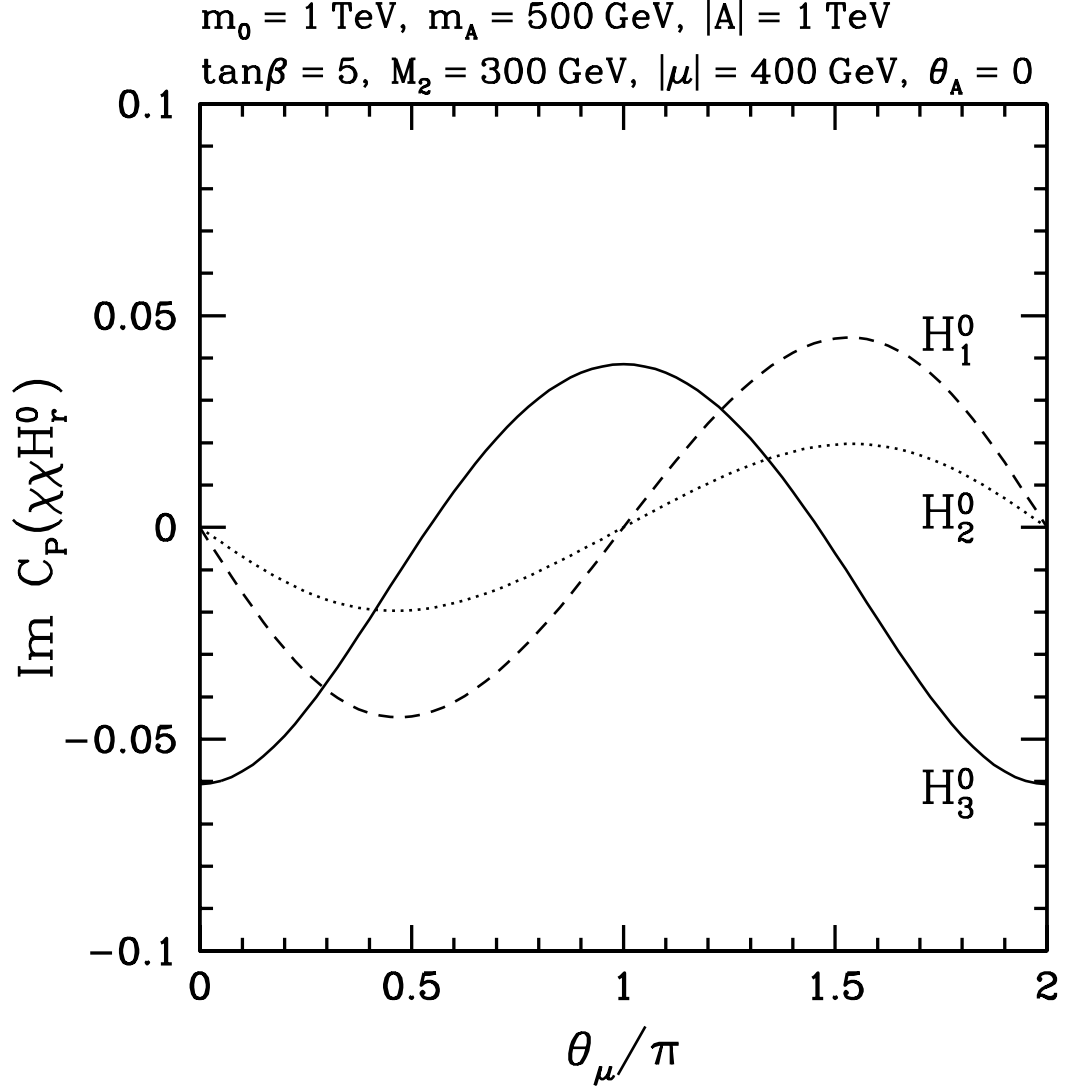


FIG. 6: The imaginary part of the pure imaginary coupling constants $C_P^{\chi\chi H_r^0}$ ($r = 1, 2, 3$) as a function of θ_μ for the same choice of parameters as Fig. 4.

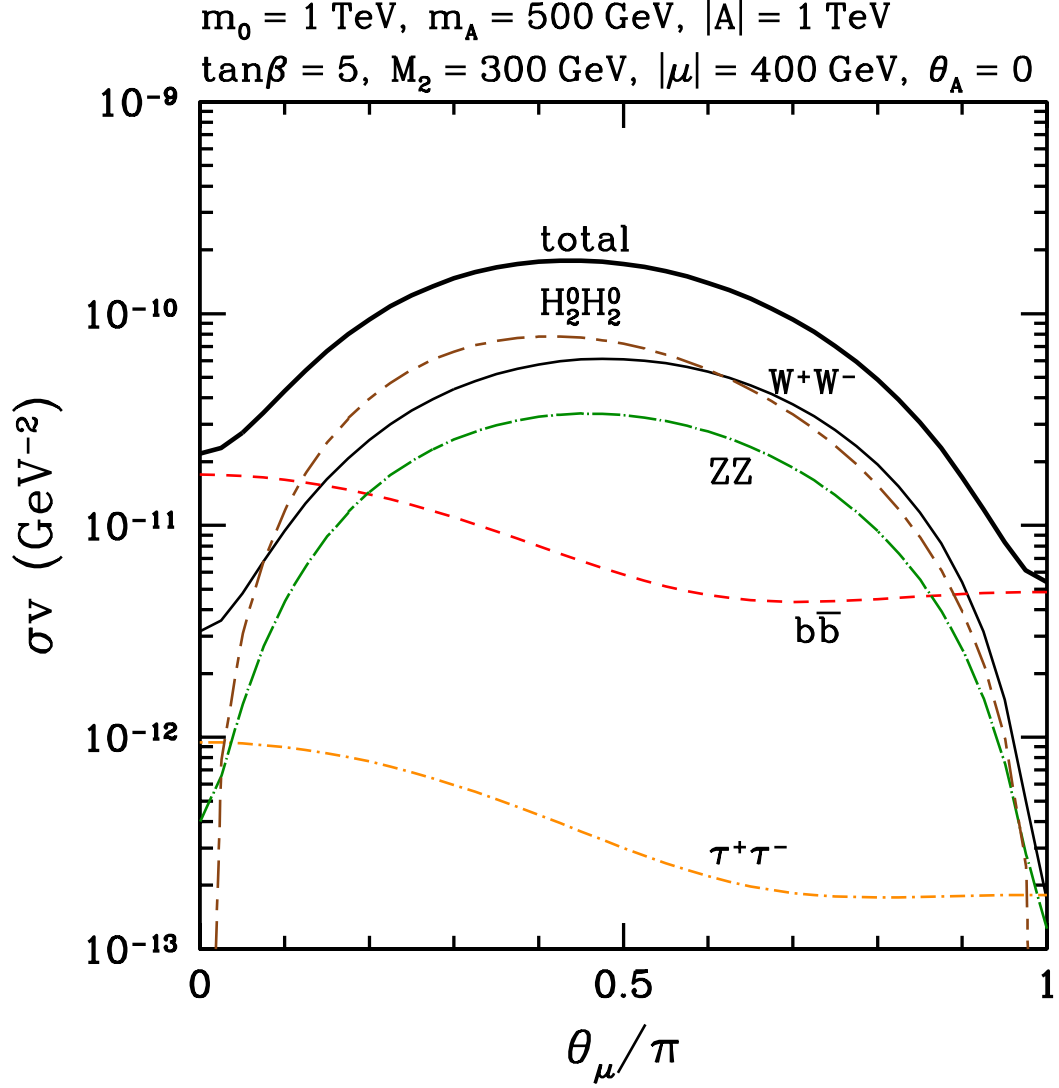


FIG. 7: The cross section times relative velocity σv for $v = 10^{-3}$ versus θ_μ for the same choice of parameters as Fig. 4. The solid, long dash-dot, short dashed, short dash-dot and short dash-long dash lines correspond to the contributions from $W^+ W^-$, ZZ , $b\bar{b}$, $\tau^+ \tau^-$ and $H_2^0 H_2^0$ final states, respectively. The bold solid line represents the sum of all the contributions.

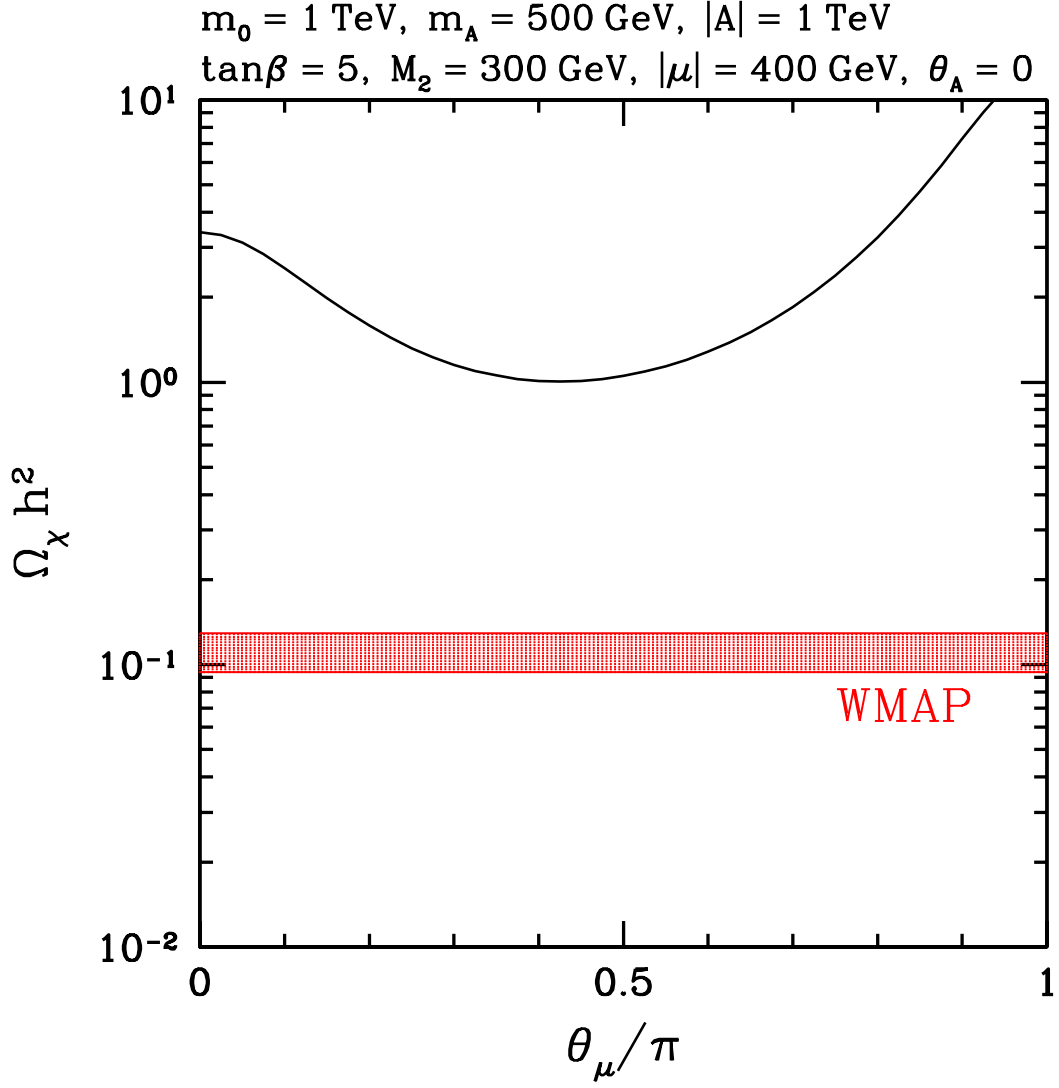


FIG. 8: The relic density $\Omega_\chi h^2$ versus θ_μ for the same choice of parameters as Fig. 4. In the shaded region, the relic density is consistent with the WMAP 2σ bound.

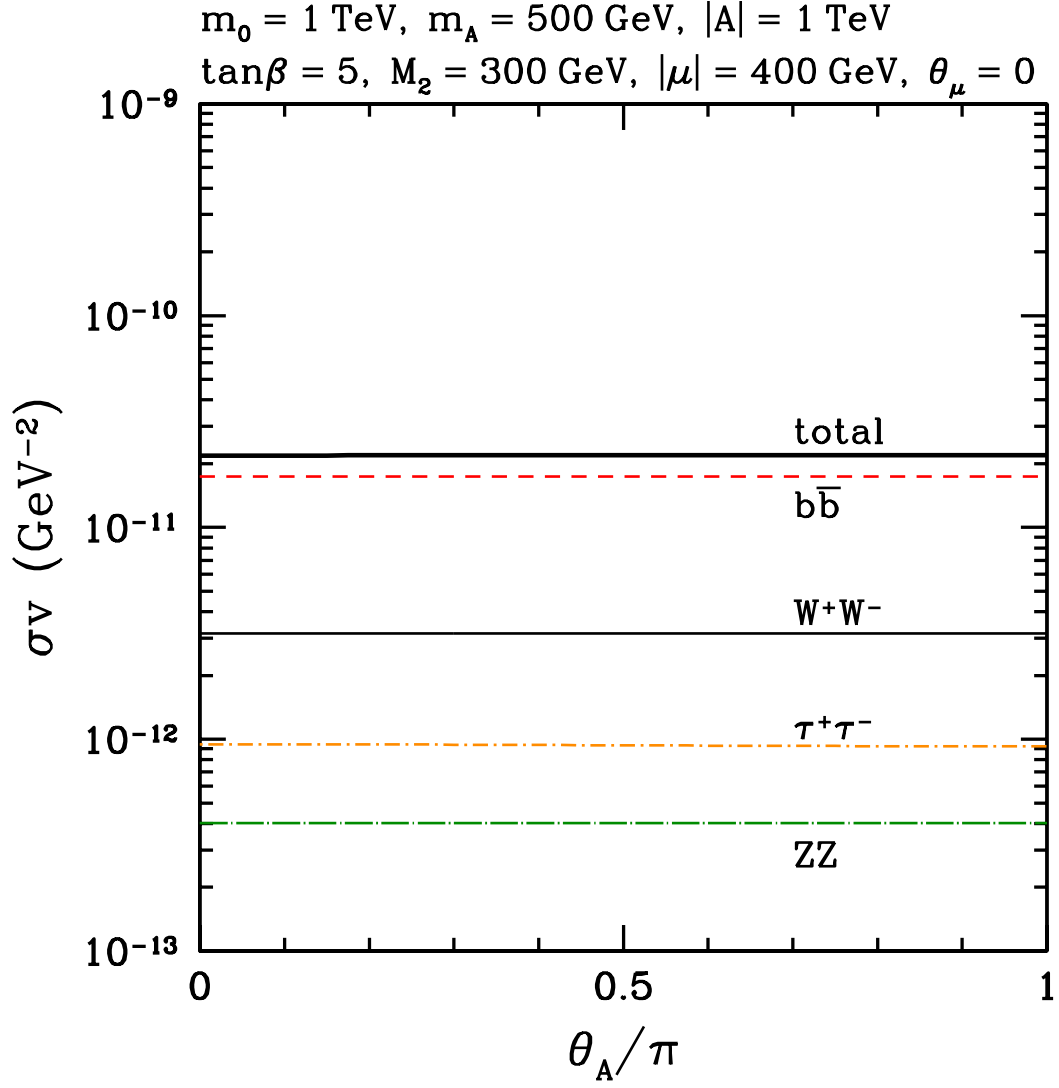


FIG. 9: The cross section times relative velocity σv for $v = 10^{-3}$ versus θ_A for the same choice of parameters as Fig. 4 but $\theta_\mu = 0$.

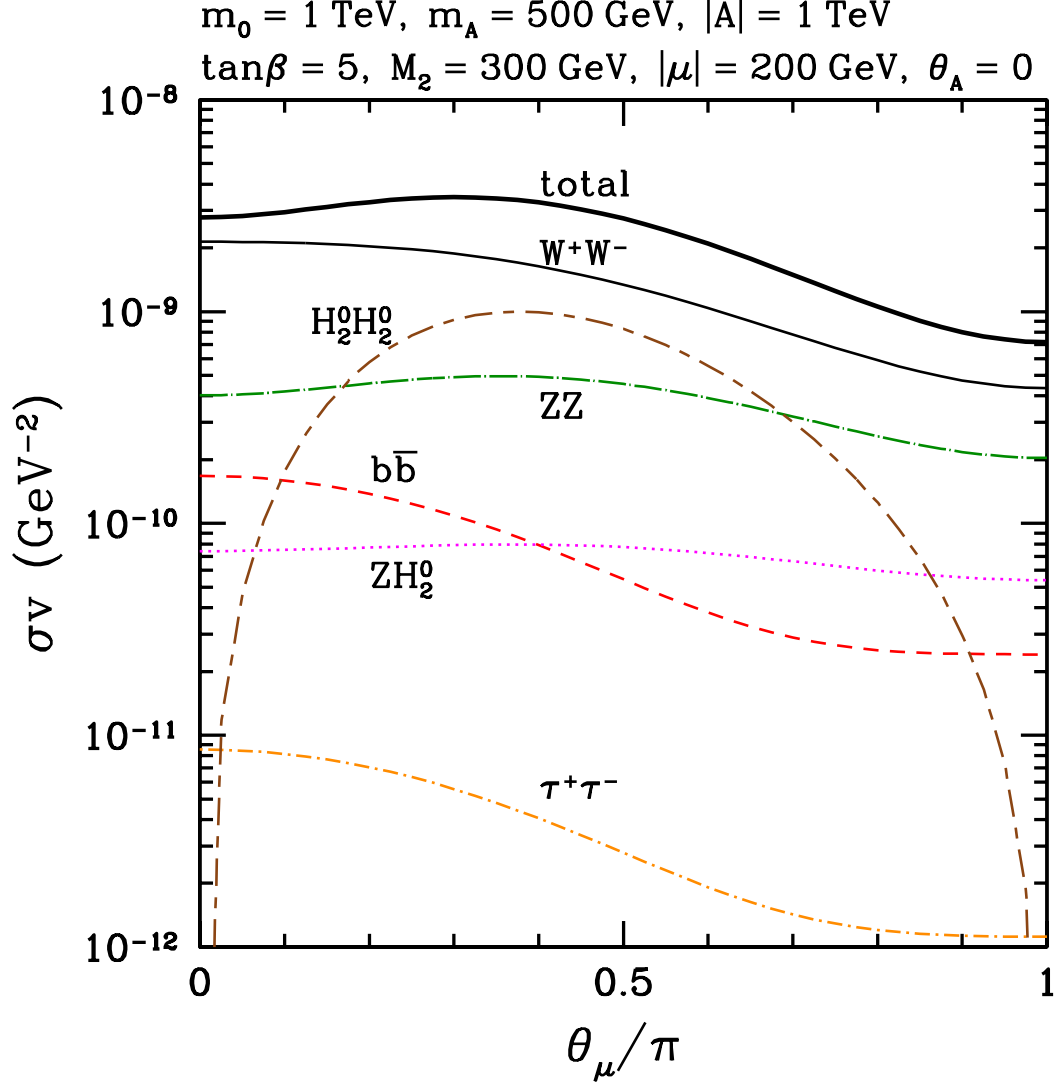


FIG. 10: The cross section times relative velocity σv for $v = 10^{-3}$ versus θ_μ for $M_2 = 300 \text{ GeV}$ and $|\mu| = 200 \text{ GeV}$. The values of the other parameters are the same as Fig. 4. The solid, long dash-dot, short dashed, long dashed, short dash-dot, short dash-long dash and dotted lines correspond to the contributions from W^+W^- , ZZ , $b\bar{b}$, $t\bar{t}$, $\tau^+\tau^-$, $H_2^0 H_2^0$ and ZH_2^0 final states, respectively. The LSP in this case is a mixture of the bino and the higgsinos.

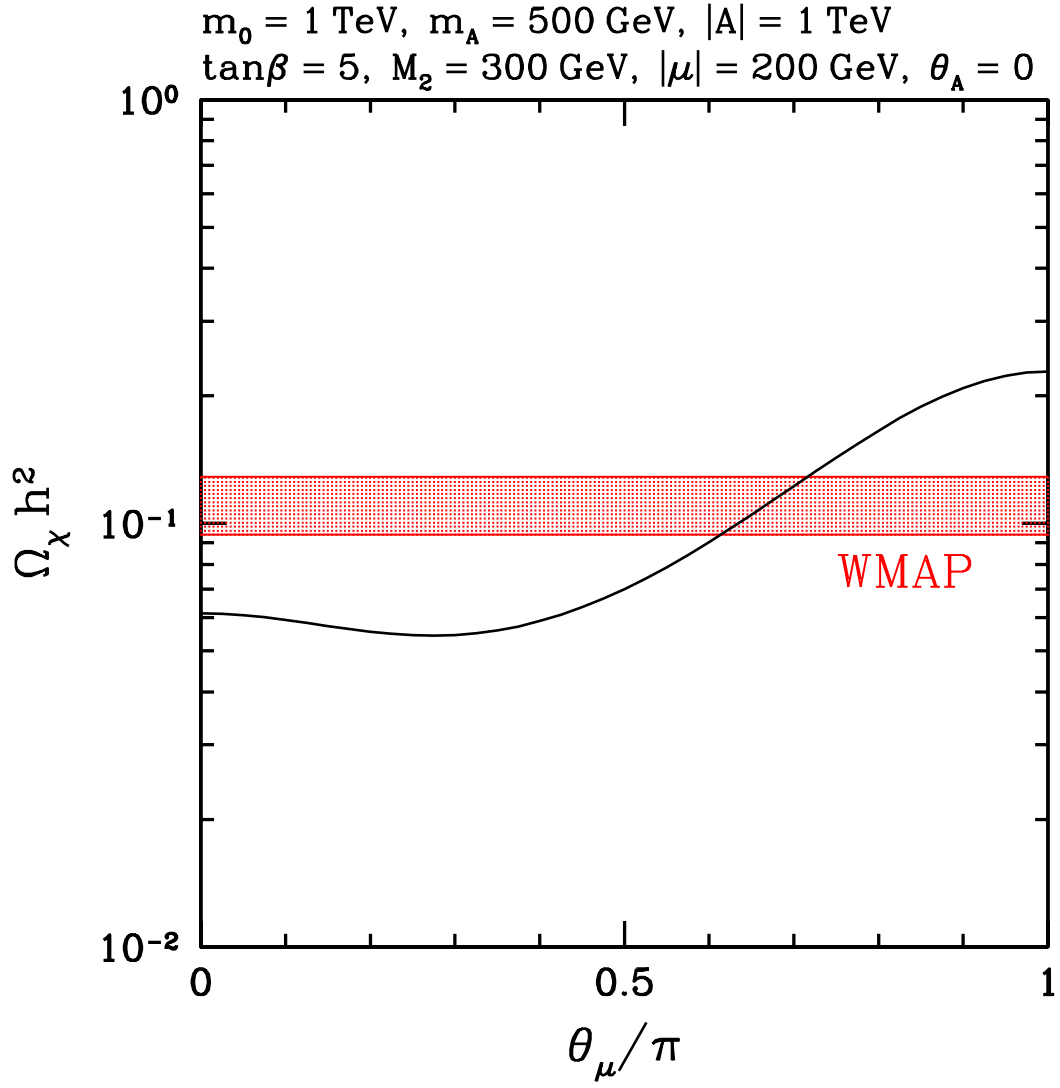


FIG. 11: The relic density $\Omega_\chi h^2$ versus θ_μ for the same choice of parameters as Fig. 10.

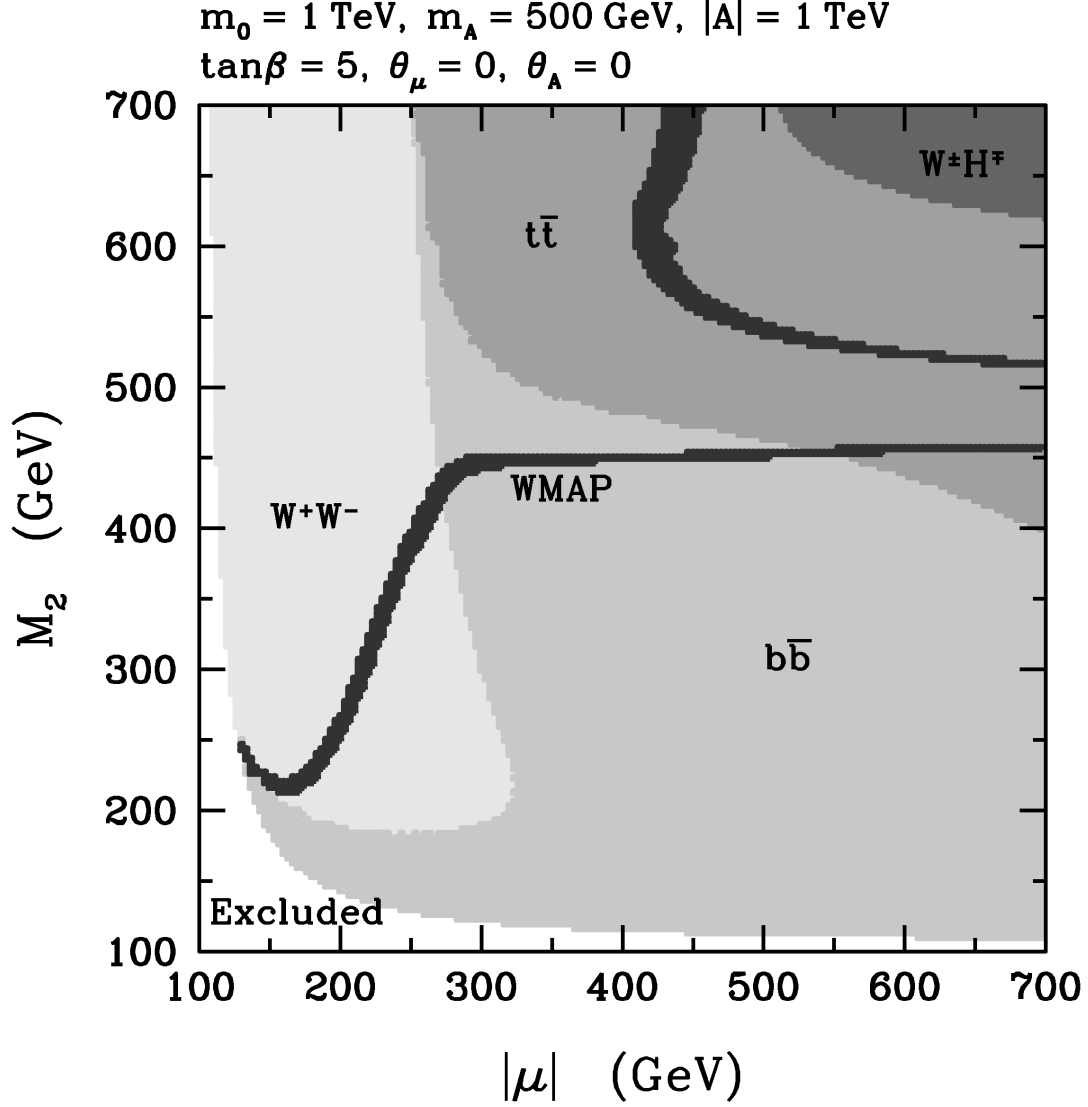


FIG. 12: The final states giving the largest contribution to σv for $v = 10^{-3}$ in the $(|\mu|, M_2)$ plane for $m_0 = |A| = 1 \text{ TeV}$, $m_A = 500 \text{ GeV}$, $\tan\beta = 5$, $\theta_A = 0$ and $\theta_\mu = 0$. The regions where the final states W^+W^- , $b\bar{b}$, $t\bar{t}$ and $W^\pm H^\mp$ give the largest contribution are shown in different gray scales. From lighter to darker, each region corresponds to W^+W^- , $b\bar{b}$, $t\bar{t}$ and $W^\pm H^\mp$ in this order. In the darkest strip, the relic density is consistent with the WMAP 2σ result. The white region is excluded by the LEP limit on the chargino mass $m_{\chi_1^\pm} > 104 \text{ GeV}$ [49] and the lightest Higgs mass $m_{H_2^0} > 113 \text{ GeV}$ [50].

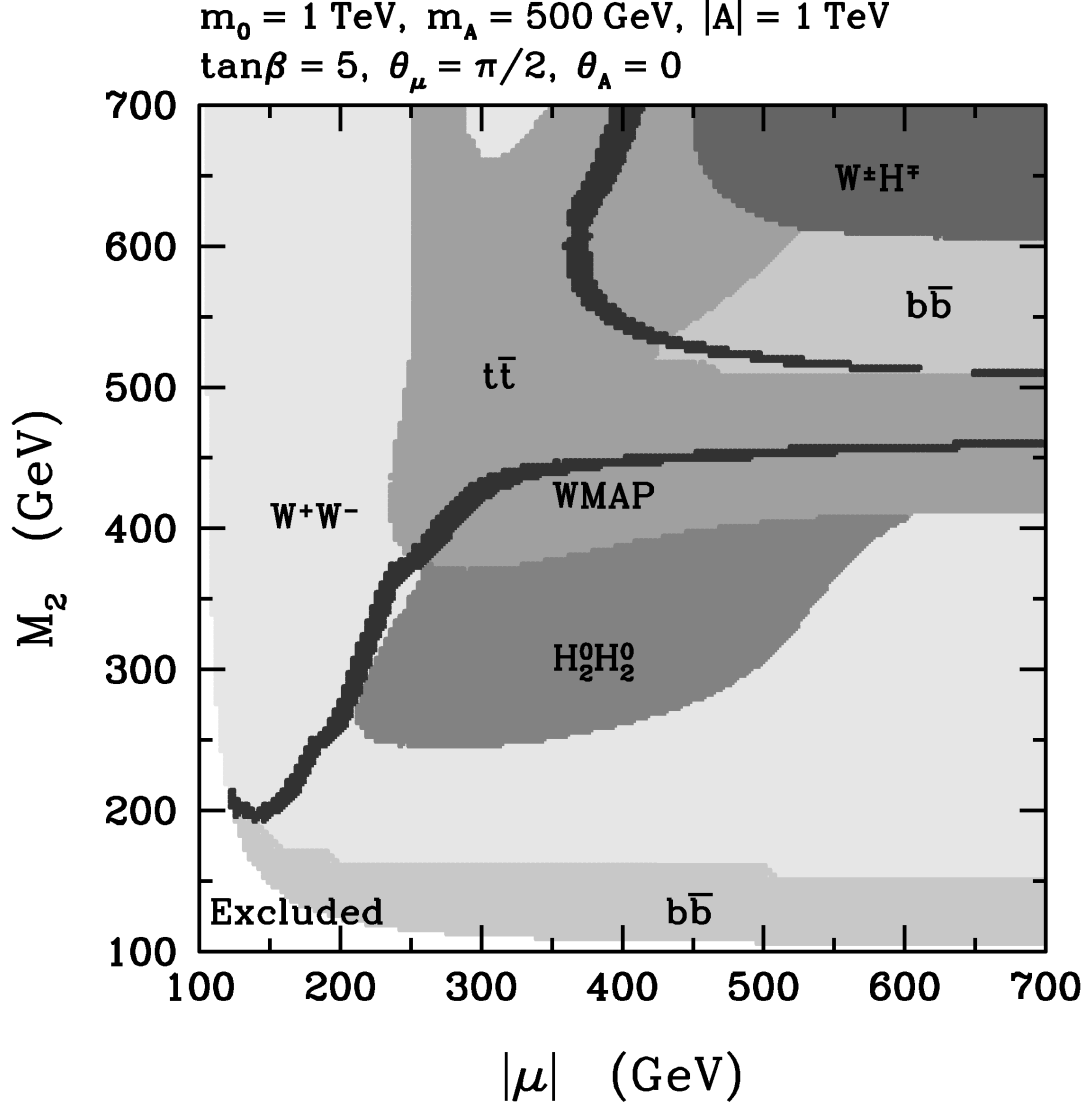


FIG. 13: The same as Fig. 12 but for $\theta_\mu = \pi/2$. The regions where the final states W^+W^- , $b\bar{b}$, $t\bar{t}$, $H_2^0 H_2^0$ and $W^\pm H^\mp$ give the largest contribution are shown in different gray scales. From lighter to darker, each region corresponds to W^+W^- , $b\bar{b}$, $t\bar{t}$, $H_2^0 H_2^0$ and $W^\pm H^\mp$ in this order.

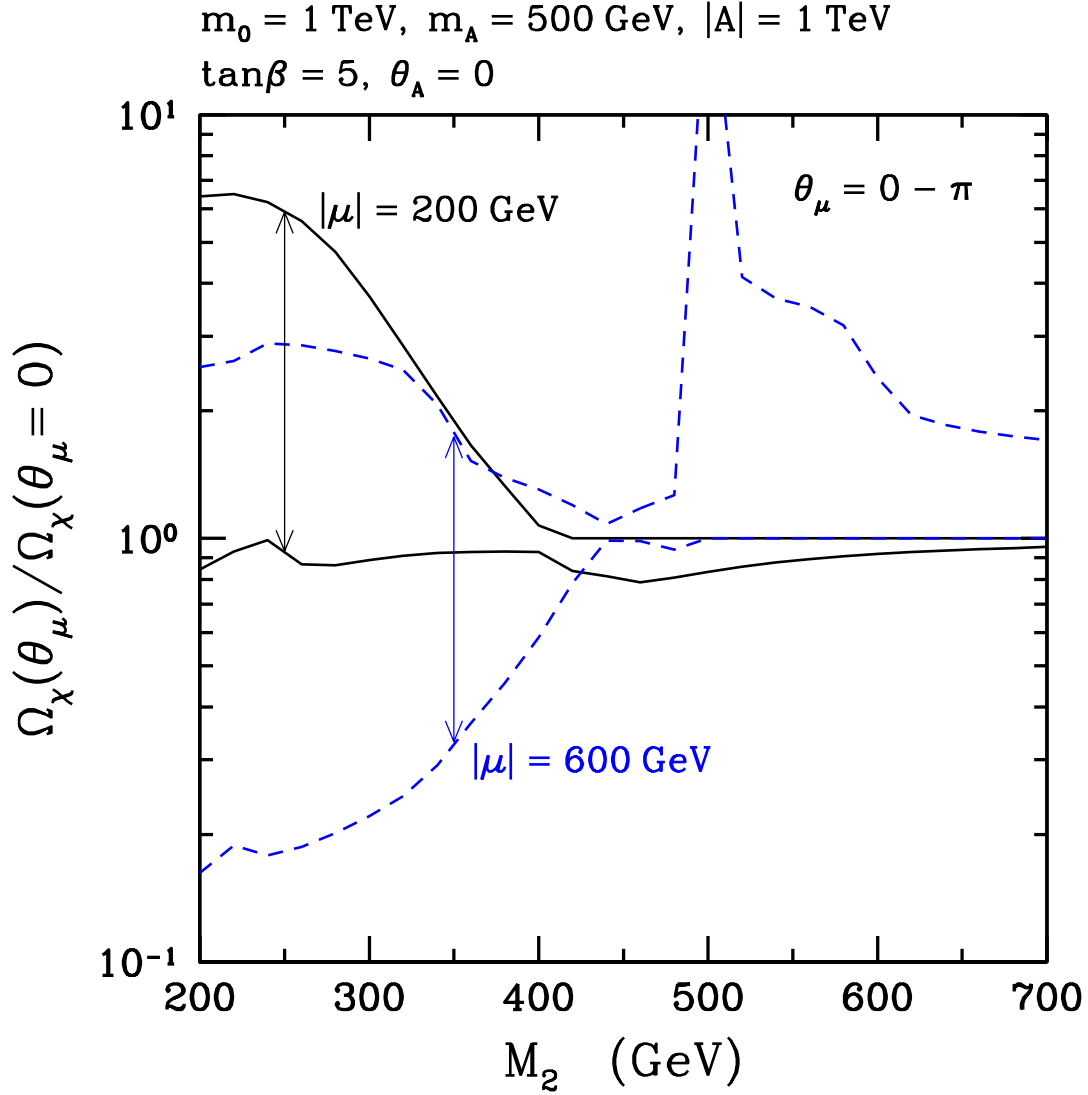


FIG. 14: Variation of the relic density with θ_μ normalized by that for $\theta_\mu = 0$, $\Omega_\chi(\theta_\mu)/\Omega_\chi(\theta_\mu = 0)$, as a function of M_2 for $m_0 = |A| = 1 \text{ TeV}$, $m_A = 500 \text{ GeV}$, $\tan\beta = 5$ and $\theta_A = 0$. Varying θ_μ in the range $0 < \theta_\mu < \pi$, the relic density lies between the two solid lines for $|\mu| = 200 \text{ GeV}$. The region between the two dashed lines represents the corresponding result for $|\mu| = 600 \text{ GeV}$.

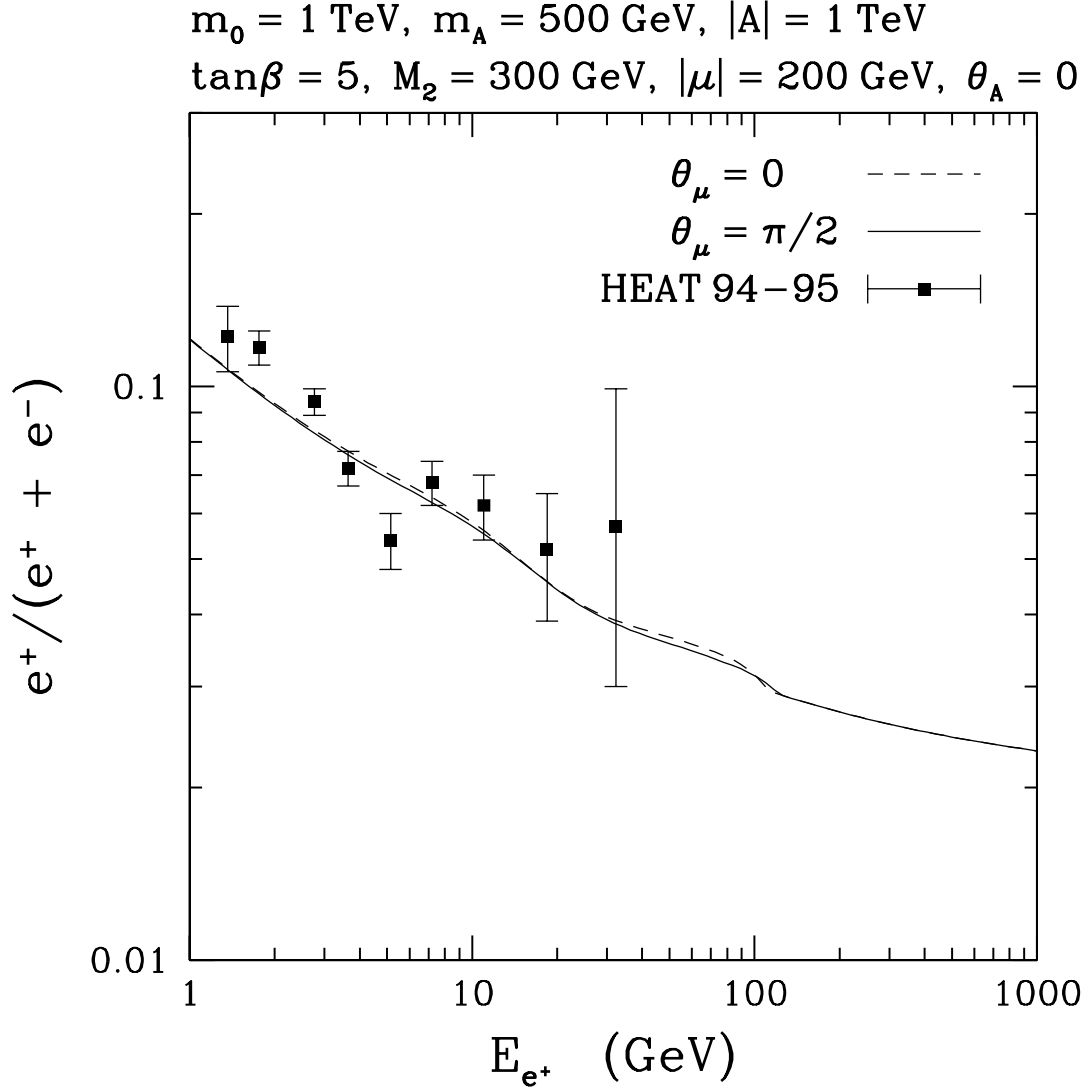


FIG. 15: Positron fraction $e^+/(e^+ + e^-)$ versus positron energy E_{e^+} for the same choice of parameters as in Fig. 10. The dashed and solid lines correspond to the results for $\theta_\mu = 0$ and $\theta_\mu = \pi/2$, respectively. The points with error bars represent the data from HEAT measurement [42].

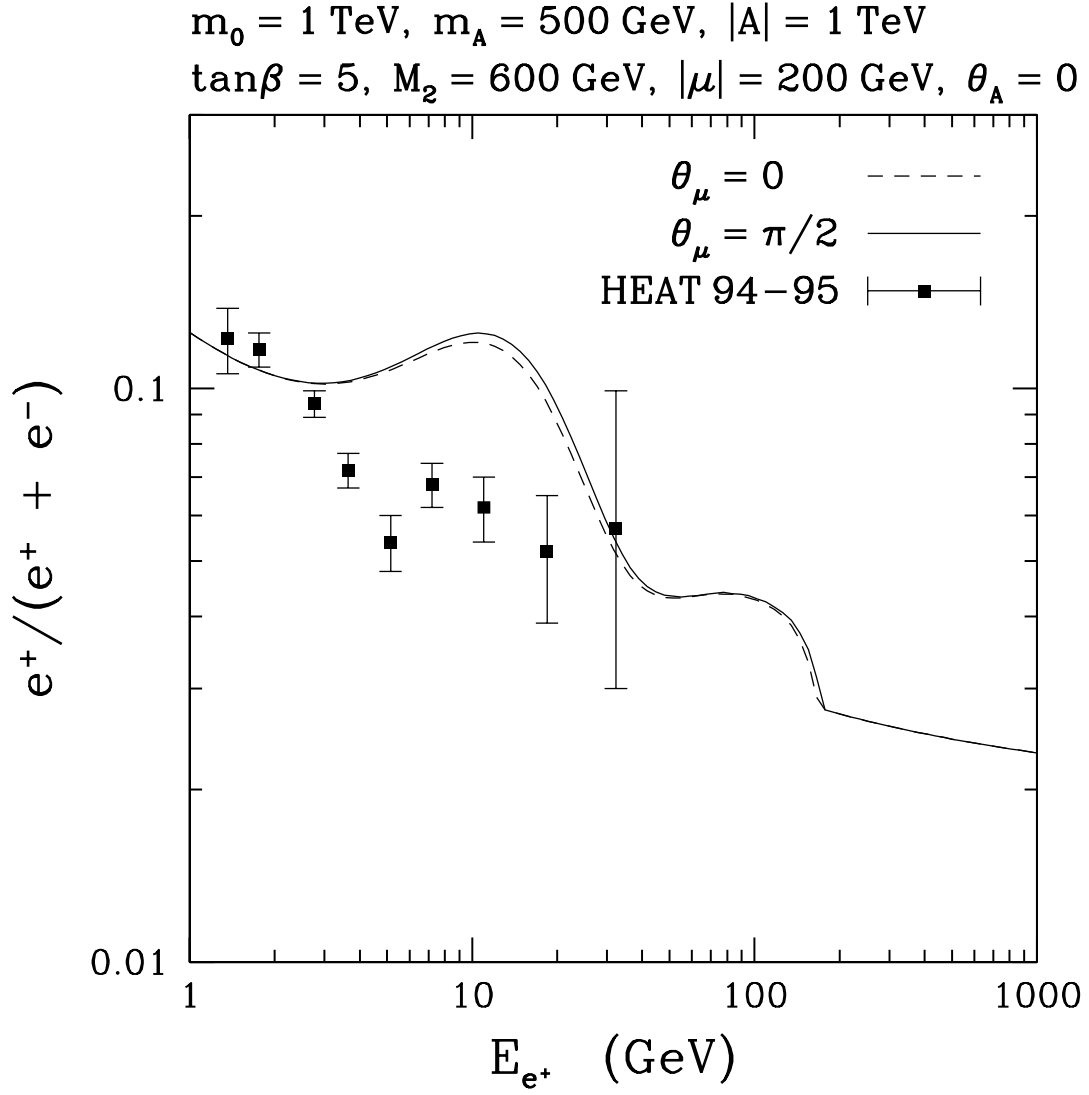


FIG. 16: The same as Fig. 15 but for $M_2 = 600 \text{ GeV}$. The LSP in this case is higgsino-like.